Elsevier Editorial System(tm) for Marine and Petroleum Geology

Manuscript Draft

Manuscript Number: JMPG-D-15-00306R1

Title: INCREASING THE PREDICTIVE POWER OF GEOSTATISTICAL RESERVOIR MODELS BY INTEGRATION OF GEOLOGICAL CONSTRAINTS FROM STRATIGRAPHIC FORWARD MODELING

Article Type: Full Length Article

Keywords: Stratigraphic Forward Models (SFM); geostatistics; reservoir simulation; data integration; uncertainty propagation

Corresponding Author: Dr. Quinto Renato Sacchi, Ph.D.

Corresponding Author's Institution: Politecnico di Torino

First Author: Quinto Renato Sacchi, Ph.D.

Order of Authors: Quinto Renato Sacchi, Ph.D.; Eloisa Salina Borello; Gert Jan Weltje, Prof.; Rory Dalman, Ph.D.

Abstract: Current static reservoir models are created by quantitative integration of interpreted well and seismic data through geostatistical tools. In these models, equiprobable realizations of structural settings and property distributions can be generated by stochastic simulation techniques. The integration of regional (or basin) scale knowledge in reservoir models is typically performed qualitatively or semi-quantitatively (for example, through the definition of regional property trends or main channel-belt orientations). This limited use of regional information does not allow an assessment of the impact of the uncertainties associated with the regional knowledge on the overall uncertainty of the reservoir model.
A novel approach is proposed in this study, which allows us to consistently integrate basin-scale information into reservoir models. A new type of data, related to the distribution of the potential hydrocarbon-bearing volumes at basin scale, was obtained from a 2-DH process-based stratigraphic forward model (SFM) and integrated as a soft constraint in the geostatistical reservoir modeling. As a consequence, reservoir models are quantitatively consistent with the large-scale geological setting defined by the SFM output. Furthermore, the uncertainty associated with each SFM parameter can be propagated to reserve estimation. Thus the partitioning of the overall uncertainty affecting a reservoir model into the contributions of the uncertainties at the basin and reservoir scales can be quantitatively assessed. Several synthetic case studies were carried out with and without conditioning to SFM output, which verified the effectiveness of the method. A logical next step is to apply the proposed methodology to a real-world case.

POLITECNICO DI TORINO

petroleum engineering group

Dott. Quinto Sacchi

Turin, 14/10/2015

To: the Executive Managing Editor
Marine And Petroleum Geology

Subject: **Revised manuscript submission**

Dear Editor,

We would like to submit the revised manuscript for publication: "INCREASING THE PREDICTIVE POWER OF GEOSTATISTICAL RESERVOIR MODELS BY INTEGRATION OF GEOLOGICAL CONSTRAINTS FROM STRATIGRAPHIC FORWARD MODELING"

Corresponding author: Quinto Sacchi
Address: DITAG Department, Politecnico di Torino, C.so Duca degli Abruzzi 24, 10129, Turin, Italy.
Telephone number : 0039-011-0907730
Fax number : 0039-011-0907699
Email: quinto.sacchi@polito.it

We affirm that the manuscript has been prepared in accordance with the Guide for Authors.

We hereby affirm that the content of this manuscript or a major portion thereof has not been published in a refereed journal, and it is not being submitted for publication elsewhere.

Type of Manuscript : Research paper

Sincerely yours,
Quinto Sacchi

Department of Environment, Land and Infrastructure Engineering

Politecnico di Torino – Department of Environment, Land and Infrastructure Engineering (DIATI)
Corso Duca degli Abruzzi, 24 – 10129 Torino Italia
Tel: +39 011 090 7730; fax: +39 011 090 7699
e-mail: quinto.sacchi@polito.it url: www.polito.it/petroleum

***Detailed Response to Reviewers (Revision Notes)**

We greatly acknowledge the reviewers valuable comments. We addressed them.

Reviewer #1:

I recommend you to add a **nomenclature** list for clarity.
Done (page 20)

I also suggest to shorten the second part of the introduction, and integrate the left out parts into the Methodology section.
The introduction was significantly shorten(pages 4); methodological details were moved to section 2 and 2.3).

Moreover, notice that on page 10, line 21 "**marginal distribution**" is introduced but the definition is not given until line 45.
The definition of marginal distribution was introduced at the first occurrence.

Finally, axis labels should be added to hystograms in Figure 8.
Done

Reviewer #2:

A question immediately raised here is **why not a real case study is used**. Perhaps the authors could add some comments on this, as most potential users would find this more realistic and useful.
We intend to apply the methodology to a real-world case in a follow-up study.

However, the paper as it stands is fully acceptable with minor modifications, one of which concerns **equation 2** which is erroneous.
Corrected

There are a few grammatical, technical and graphical minor changes I suggest and which I annotated on a paper copy which I can hand over to one of the co-authors (no. 3) whom I will meet on a PhD defence shortly.
Corrected

Highlights:

- Stratigraphic Forward Model (SFM) provides channel body volumetrics at basin scale
- Basin-scale constraints from the SFM were integrated into reservoir models
- Uncertainty of basin-fill parameters was propagated to reserve estimation
- Inference of basin-fill parameters from reservoir data reduced their uncertainty

INCREASING THE PREDICTIVE POWER OF GEOSTATISTICAL RESERVOIR MODELS BY INTEGRATION OF GEOLOGICAL CONSTRAINTS FROM STRATIGRAPHIC FORWARD MODELING

Quinto Sacchi[1*], Eloisa Salina Borello[1], Gert Jan Weltje[2], Rory Dalman[3]

[1] **Politecnico di Torino**, Department of Environment, Land and Infrastructure Engineering, Corso Duca degli Abruzzi 24, 10129 Torino, Italy.

[2] **University of Leuven**, Department of Earth and Environmental Sciences, Celestijnenlaan 200E, 3001 Leuven-Heverlee, Belgium.

[3] **TNO,** Netherlands Organisation for Applied Scientific Research, Princetonlaan 6, 3584CB Utrecht, The Netherlands.

Keywords: Stratigraphic Forward Models (SFM); geostatistics; reservoir simulation; data integration; uncertainty propagation

Highlights:

- Stratigraphic Forward Model (SFM) provides channel body volumetrics at basin scale
- Basin-scale constraints from the SFM were integrated into reservoir models
- Uncertainty of basin-fill parameters was propagated to reserve estimation
- Inference of basin-fill parameters from reservoir data reduced their uncertainty

* **Corresponding author**: Corso Duca degli Abruzzi 24, 10129 Torino, Italy; E-mail: quinto.sacchi@polito.it; phone: +390110907730; fax: +390110907699;

ABSTRACT

Current static reservoir models are created by quantitative integration of interpreted well and seismic data through geostatistical tools. In these models, equiprobable realizations of structural settings and property distributions can be generated by stochastic simulation techniques. The integration of regional (or basin) scale knowledge in reservoir models is typically performed qualitatively or semi-quantitatively (for example, through the definition of regional property trends or main channel-belt orientations). This limited use of regional information does not allow an assessment of the impact of the uncertainties associated with the regional knowledge on the overall uncertainty of the reservoir model.

A novel approach is proposed in this study, which allows us to consistently integrate basin-scale information into reservoir models. A new type of data, related to the distribution of the potential hydrocarbon-bearing volumes at basin scale, was obtained from a 2-DH process-based stratigraphic forward model (SFM) and integrated as a soft constraint in the geostatistical reservoir modeling. As a consequence, reservoir models are quantitatively consistent with the large-scale geological setting defined by the SFM output. Furthermore, the uncertainty associated with each SFM parameter can be propagated to reserve estimation. Thus the partitioning of the overall uncertainty affecting a reservoir model into the contributions of the uncertainties at the basin and reservoir scales can be quantitatively assessed.

Several synthetic case studies were carried out with and without conditioning to SFM output, which verified the effectiveness of the method. A logical next step is to apply the proposed methodology to a real-world case.

1 INTRODUCTION

Geological reservoir modeling encompasses all aspects related to the definition of the structural, stratigraphic, lithological and petrophysical properties of subsurface rocks, leading to the estimation of the spatial distribution and the volume of hydrocarbons in place (Mallet, 2002).

Available information for geological reservoir modeling includes static and dynamic data at different scales (Fig.1), ranging from centimeters (core data) to kilometers (2D/3D seismic). Typically, reservoir models result from the quantitative integration of available static data, i.e. well logs, core data and seismic data (Cosentino, 2001, Benetatos and Viberti, 2010). These kinds of data are complementary because well data are characterized by high vertical resolution (log sampling is usually in the order of decimeters) and low horizontal resolution (well spacing is usually some hundreds of meters to some kilometers and wells are not uniformly distributed), whereas seismic data is characterized by relatively high horizontal resolution (tens of meters) and low vertical resolution (tens of meters). In creating static reservoir models, depth horizons derived from seismic data provide the structural description, whereas well logs give information about the vertical distribution of reservoir lithologies.

Generally, due to the low density of wells in the oil industry, the vertical trend corresponding to the average proportional abundance of lithofacies encountered in the wells is assigned to the entire domain in the form of a vertical proportion curve. This assumption of stationarity assumes that statistics from wells are representative of the 3D field properties. However, stationarity cannot be easily justified from a sedimentological point of view, and the extent to which vertical proportion curves represent the actual mean lithofacies abundances depends strongly on the number and pattern of wells (Massonnat, 1999). Approaches based on stationary random functions therefore often lead to inaccurate reservoir models (Labourdette et al., 2008).

If the stationarity hypothesis does not hold true in the volume of interest, additional geological information should be incorporated into the modeling workflow to constrain stochastic simulations. Several approaches have been developed during recent years to quantify the lateral variability of reservoir lithology: (1) Information extraction from seismic surveys (e.g. Beucher et al., 1999; Marion et al., 2000; Strebelle et al., 2003; Zachariassen et al., 2006); (2) Building of a 3D paleobathymetry grid from sedimentological well

data (Massonnat, 1999); (3) Using analogous geological situations (Howell et al., 2014); (4) Integrating dynamic data, such as well-test interpretation and production data (e.g. Oliver, 1994; Wen et al., 1998); (5) Integrating sedimentological cross sections (Labourdette, 2008), and (6) incorporating local prior probability in stochastic reservoir simulation (e.g. Deutsch, 2002; Mallet, 2002).

In this study we propose a novel methodology to quantitatively integrate basin-scale information into reservoir models and account for the associated uncertainty. The proposed methodology allows the construction of a quantitative prior 3D probability cube of lithology (or lithofacies) proportions, by introduction of additional basin-scale information, not extractable from either well or seismic data, but obtainable from stratigraphic forward models (SFMs). In a previous study (Sacchi et al., 2015) we illustrated how the most likely scenarios could be selected from a series of SFM realizations by an objective function which quantifies the discrepancy between the actual and predicted elevation of a regional seismic reflector corresponding to the reservoir top. In the present study, we show that the SFM constraints permit us to reconstruct a geological reservoir model by geostatistical techniques, which may be used to downscale the results of the SFM to the reservoir grid. In particular, we show that we can successfully interpolate the local information derived from well logs by imposing a spatial correlation expressed in terms of covariance. The uncertainty associated with spatial prediction is modeled by random function theory. In a follow-up study, we intend to apply the methodology proposed by Sacchi et al. (2015) and the present study to a real-world case.

2 METHODOLOGY

The workflow proposed in this study aims at integrating typical data sets used for geological reservoir modeling, made up of well and seismic data, with a potentially new kind of data, represented by the parameters estimated by a quantitative Stratigraphic Forward Model (SFM). The SFM provides the channel-belt architecture at basin scale, which can be expressed as a non-stationary 3D probability distribution of depositional lithofacies proportions. This probability cube was used as additional input for the geostatistical reservoir model. The proposed workflow was applied to a fluvio-deltaic environment.

Two geostatistical approaches are in widespread use for modeling reservoirs in fluvio-deltaic environments (Daly and Caers, 2010), namely Object-Based Facies Modeling (OBFM) (Georgsen et al., 1994) and Multiple-Point Statistics (MPS) (Strebelle, 2002). The first technique directly addresses the issues of geometry and connectivity, producing a model that contains explicit representations of the channel features conditioned to data. However, in some circumstances conditioning to data can be difficult, for example with dense well data sets or with multiple soft probability fields (Tetzlaff et al., 2005; Strebelle, 2012; Caers and Zhang, 2004). The second technique complements traditional variogram driven cell-based modeling as well as the object modeling approach. In fact, it is a cell-based approach that uses a training image to estimate the multivariate distribution of quantities of interest, instead of a variogram-based algorithm that expresses a simple bivariate distribution. Both approaches were considered in this study, and their ability to integrate basin data whilst preserving realistic geometry was analyzed and compared.

Incomplete information on the geological features and geophysical parameters characterizing the subsurface induces uncertainty in every aspect and in every phase of reservoir geological modeling (Caers, 2005). Uncertainty of the integrated basin information was taken into account and propagated to the reservoir scale. The proposed workflow is summarized in Figure 2, and is described in detail in the following subsections.

2.1 Stratigraphic Forward Model

For basin-scale simulation an aggregated, 2DH (depth-averaged flow in the two-dimensional horizontal plane) stratigraphic model, called SimClast (Dalman and Weltje, 2008, 2011) was adopted. SimClast was developed from 2005 to 2008 at Delft University of Technology (Netherlands) to study the complex interactions between fluvial and wave influences on deltaic and shore-face development. SimClast features, relevant for this study, are: realistic channel network development, channel stability based on dynamic calculation of super elevation, and sub-grid parametrization of channel features governing avulsions and floodplain aggradation. The term sub-grid parameterization originated in the field of computational fluid dynamics (Meneveau, 2010). In the context of this study, it refers to the implementation of small-scale processes which govern the evolution of drainage networks (such as avulsions) as sub-grid scale routines into the large-scale basin-filling model. In SimClast the subgrid parametrization of alluvial processes and

stratigraphy is performed to incorporate the small-scale processes and stratigraphic/architectural elements into the large-scale 2DH stratigraphic model, resulting in the level of vertical detail required for geological reservoir modeling with a moderate amount of computational effort.

In order to perform one simulation with SimClast several environmental parameters have to be set: the initial surface and subsurface sediment properties, the sea level change, the (spatially variable) subsidence, the river inflow location, the discharge and sediment supply over the runtime, the wave regime, and the current pattern at the grid boundaries (Dalman and Weltje, 2011). As in the previous study (Sacchi et al., 2015), our main focus was on the analysis of the impact of the variation of three environmental parameters that have the largest influence during the geologically short time interval simulated (ca. 8000 years): (1) initial topography, (2) sea level and (3) sediment entry point. The other parameters were assumed to be known and constant. Each model run was conducted under time-invariant forcing, i.e. constant sea level, liquid discharge and sediment load. Two discrete sediment classes were considered: sand, mostly deposited in and near fluviodeltaic channels, and clay, representative of the floodplain and shallow-marine plume deposits.

2.2 Channel-belt architecture at basin scale

When a SimClast basin simulation is run, output is generated in the form of multiple maps (snapshots) of topography, sedimentation patterns and discharge. Furthermore, a 3D cube of discrete stratigraphic data of sediment thickness, grain size and age is created for the entire area. The information related to channel architecture was extracted from the sub-grid parameterization of the fluvio-deltaic architecture, which specifies channel patterns in terms of volume of channelized deposits, flow direction and channel top for each grid node (x, y).

The fluvial architecture is constrained to the horizontal discretization of the SFM. The horizontal dimension of the grid cells in the reservoir model is one order of magnitude below that of the SFM; this implies that lithological variability at the basin scale obtained by the SFM should be regarded as spatially averaged information at the reservoir scale. In particular, channels are assumed to have a smaller width than

the cell dimension (Dalman and Weltje, 2008), thus their exact location cannot be resolved at basin scale, nor is it possible to determine the width to thickness (W/T) ratio of the channels inside each cell generated by the SFM.

The sub-grid information was extracted to obtain a 3D distribution of *channel occurrence probability* at basin scale. This information was integrated as a soft constraint in the geostatistical simulation which complies with the uncertainty related to the exact channel position at reservoir scale.

The channel occurrence probability for each location (x, y, z) was calculated as follows:

$$P_{CH}(x, y, z) = \frac{V_{CH}}{V_{cell}} \tag{1}$$

where V_{CH} is the channel volume in position (x, y, z) while V_{cell} represents the grid cell volume. Channel occurrence probability (P_{CH}) was assumed to be constant along the channel thickness (h).

Since the subgrid parameterization does not supply any information about channel width, length or thickness, the latter was estimated from the channel volume, given a W/T ratio (f):

$$h(x, y, z) = \sqrt{\frac{V_{CH}}{l_{CH} f}} \tag{2}$$

where l_{CH} (channel length) was approximated with the cell extension Δx. The W/T ratio employed equals 250, a representative value for distributary channels and crevasse deposits (Reynolds, 1999).

2.3 Reservoir realizations constrained to basin information

For each SFM scenario several equiprobable stochastic reservoir scenarios were generated, both with the multiple-point geostatistical approach and the object-based facies modeling approach. In other words, each vector of SFM input parameters (sea level, initial topography and sediment entry point) generated several reservoir realizations, which were expressed in terms of spatial lithology distribution over the reservoir-scale grid. This approach was followed in order to capture the uncertainty associated with the downscaling of each scenario to the reservoir-scale grid.

The geostatistical approach provides a weighted integration of the different kinds of data (Daly and Caers, 2010). Well data, in the form of lithology logs previously defined, are classified as 'hard' data because they derive from the interpretation of direct measurements. Well stratigraphy constitutes a strong constraint during model building and it is integrated into the model without any modification. The depth horizons derived from seismic data interpretation were also assumed to be fixed (i.e. equal for all realizations). Conversely, local basin information was integrated as soft constraining data: the distribution of channel volume fraction at basin scale was softly imposed as a volume trend. In other words, the information arising from SFM simulation was converted into a 3D probability cube of lithology proportions and locally imposed at each grid cell.

Basin-scale averaged information, such as the overall channel volume fraction and the main channel orientation, was also integrated. In the multiple-point geostatistical approach the overall sand fraction and main channel orientation was integrated in the training image: different training images were constructed based on the sand fraction and channel orientation obtained by different SFM scenarios. In the object-modeling approach the sand fraction and channel orientation are required parameters. Channel orientation was assumed normally distributed with a mean equal to the mode of the SFM simulations and a fixed standard deviation (45°), corresponding to the highest SFM resolution, was imposed. The remaining parameters were taken from literature (Reynolds, 1999; Gibling, 2006): amplitude and wavelength were assigned a triangular distribution with given minimum, mean and maximum values. The W/T ratio was fixed at 250; the width was triangularly distributed with a minimum value equal to 300 m, a mean value of 450 m and maximum value of 600 m.

2.4 Uncertainty at basin scale

A reasonable degree of uncertainty was imposed on each of the three considered SFM parameters (Sacchi et al., 2015). A range of variability for sea level and location of the sediment entry point was assumed. Several initial topographies at basin scale were stochastically generated by perturbing a reference initial topography and constraining the surface to the stratigraphy observed at wells. The input parameters were assumed to be independent and uniformly distributed over the chosen ranges. A systematic sampling

algorithm (Cochran, 1963) was applied to extract basin scenarios representative of the considered uncertainty. This approach differs from a classic Monte Carlo method because a quasi-random sequence in place of a random sequence is exploited in the sampling stage (Caflisch, 1998). A Quasi-Monte Carlo method requires a smaller number of samples to reach the same accuracy as a classic Monte Carlo method when the population is uniformly distributed, because it emphasizes a thorough coverage of the area of interest (Pal, 1998) and eliminates the clumping phenomenon, which is a limiting factor in the accuracy of the Monte Carlo method (Caflisch, 1998). As a consequence, the computational cost is significantly reduced. More complicated sampling approaches could also be applied, such as Latin Hypercube Models (Vose, 1996) or searching algorithms (eg. Falivene et al., 2014) but they are beyond the scope of this paper.

A SFM simulation was run for each quasi-random sample in order to account for uncertainty over basin input parameters, obtaining a 3D distribution of *channel occurrence probability* at basin scale for each scenario. Successively, the most promising scenarios were extracted by comparing the basin simulation results with the available data (i.e. depth horizons derived from seismic and well stratigraphy). Making use of the results of Sacchi et al. (2015), two goodness of fit functions were implemented, quantifying the ability of each scenario to match the available depth horizons derived from seismic and lithological logs, respectively. Details are reported in the appendix (eq. A1 and A2).

2.5 Accounting for basin uncertainty at the reservoir scale

The uncertainty associated with the spatial distribution of lithology at the reservoir scale could be estimated from the set of stochastic reservoir realizations. This is a non-trivial task because the data to be analyzed included several variables evaluated simultaneously and, thus, it represents a multivariate statistic of correlated variables (Johnson and Wichern, 2002). The realization of a property (channel occurrence in our case) over the grid is a vector of correlated variables (one for each grid point), where the correlation comes from the principle of spatial continuity, i.e. two data points close to each other are more likely to have similar values than two data points that are farther apart (Isaaks and Srivastava, 1989). In the proposed methodology such a correlation was guaranteed both at basin scale, by the SFM equations, and at reservoir scale, by the geostatistical theory.

Large data sets, such as the 3D lithofacies pattern realizations, pose serious obstacles to visual inference. It is not possible to visualize the uncertainties over the local realizations of each grid cell all together. Rather than summarizing this information by using descriptive statistics, we selected a number of representative locations to analyze. The nine selected locations (W1 – W9) follow a regular pattern in order to uniformly cover the reservoir area (Fig. 5b). The number of locations was chosen to preserve the statistical representativeness of the results, as a determined from sensitivity analysis.

Uncertainty obtained from the reservoir realizations was shown in terms of sand probability curve at the selected locations: sand probability of each scenario ($P_{sand}\,(x, y, z)$) was calculated as the mean of the local sand distribution over all the realizations of the given scenario. The local P_{sand} represents a marginal distribution, because the correlation between sand realization in other levels of the same location or at other locations were neglected in the calculation of local distribution percentiles. The local probability distributions were graphically represented by first, second and third quartiles. The lithology prediction at a given monitoring location, expressed by any significant vertical variation in sand probability, was verified by comparison against a reference case.

3 REFERENCE CASE AND SYNTHETIC DATASET

A synthetic appraisal scenario was considered, with four wells penetrating the reservoir. A SFM reference case was chosen extending for 50 km in the north-south direction and for 47 km in the east-west direction. The initial topography was generated with a general dip to the north-east; the altitude varies from 24 m to 74 m, resulting in an average slope of about 0.1%. The sea level was set equal to 44.5 m (above the actual sea level). The sediment supply was assumed to enter from an intermediate location along the west side of the model. Sedimentation was simulated over a period of 8000 years. Over the course of this comparatively short time interval (geologically speaking), the sediment entry point did not migrate laterally, the sea level was stable, and climate fluctuations as mirrored in changes of liquid and solid discharge were absent. A time step of 1 year was imposed, giving a vertical resolution of ~10 cm for the selected parameter set (in theory the SFM's vertical scale is unlimited). The selected time step is a good compromise between a reasonably

contained simulation time and a vertical resolution which has to be comparable with core and log data resolution. Figure 3a shows the vertically averaged net to gross (N/G) ratio, representing the proportion of sand. Main channel belt deposits are in yellow to red color (high N/G). The four wells A, B, C, and D, located in the model's central area, are also displayed. The area was discretized (fig. 3b) in a regular grid with cell dimensions (Δx, Δy) equal to 1 km x 1 km, representing the smallest horizontal spacing tolerated by SimClast. The corresponding grid at reservoir scale is 100 m x 100 m .

From this reference case, a synthetic data set was extracted which may be considered representative of data sets available for geological reservoir modeling. It consists of:

- The top stratigraphic surface, defined through the seismic interpretation.
- The lithology intercepted by wells A, B, C, D. Typically it is derived from the correlation of wireline logs to the core data.
- The well control points for bottom (initial topography) and top surfaces. They are typically defined from well log analysis.

A synthetic top stratigraphic surface was generated by perturbing the final topography simulated by the SFM to account for the overall seismic uncertainty:

$$S_r = S_{bc} + U_{1\sigma} U_{sgs} \qquad (3)$$

where:

S_{bc}: base case, or reference surface

$U_{1\sigma}$: depth error on the reference surface with assigned standard deviation σ=1

U_{sgs}: stochastic error surface obtained by Sequential Gaussian simulation with zero mean and unit standard deviation, conditioned to wells A, B, C, and D.

As a result, seismic data cover the entire basin area with horizontal resolution equal to 1000 x 1000 m.

In order to be consistent with the definition of the initial topographic surface, the same degree of uncertainty was considered. The initial and top stratigraphic surface quotes in correspondence of grid blocks intercepting wells were constrained to the well control points. Finally, well lithology was synthetically generated by downscaling the SFM lithologies of the cells containing wells A, B, C and D to reservoir scale

(fig. 4). Downscaling was performed by geostatistical simulation (Multiple-Point Statistics) in which the channel pattern information at basin scale was integrated by soft constraining.

4 RESULTS

4.1 Degree of integration of SFM with MPS vs. OBFM

Tests were conducted in order to identify the best geostatistical approach for integration of SFM information. Two different approaches were considered: Multiple-Point Statistics (MPS) and Object-Based Facies Modeling (OBFM). The 3D channel occurrence probability at basin scale (P_{CH}) for the reference case is shown in fig. 5a and two corresponding reservoir realizations simulated with OBFM and MPS, respectively, are shown in fig. 6 (a) and (b). Significantly different responses were observed. A volume-weighted upscaling to the basin scale of the reservoir realizations of fig. 6 was performed, obtaining the channel volume fraction at the basin scale shown in fig. 7. A quantitative comparison of the obtained channel volume fractions with the imposed channel probability distribution is shown in fig. 8 in terms of a 2D map and the distribution of the depth-averaged error. Both methods allow integration of the basin information, but Multiple-Point Statistics appears to respect the imposed constraints more accurately (fig. 8).

The degree of integration of the basin data was further analyzed by comparing the basin channel occurrence probability to the synthetic lithostratigraphy obtained at monitoring locations W1, W3, W5, W7, W9 in the two cases (fig. 9). Note that when a zero channel occurrence probability is imposed, reservoir realization obtained by MPS always exhibit clay (floodplain deposits), while OBFM sometimes exhibits a channel sand (for instance at W1,W3,W9), thus ignoring the assigned constraint. This is due to the difficulty of honoring a wide array of soft and hard constraints with the OBFM method (Hauge et al., 2007). New developments and approaches are being developed to reduce this limitation (Syversveen et al., 2011). In conclusion, the Multiple-Point Statistics proved to respect the constraints, while the Object-Based Facies Modeling was not able to honor all the soft data provided to steer the simulations. As a consequence, we used the Multiple-point Statistics modeling technique in the proposed workflow.

4.2 Lithology prediction at reservoir scale

Further analyses were performed to monitor the local sand probability distribution at reservoir scale obtained by geostatistical realizations constrained to the SFM reference case. A comparison of the reference case with geostatistical reservoir models obtained without any basin-scale SFM constraints was also performed to verify the effectiveness of the proposed workflow relative to the standard methodology, which only relies on seismic and well data. For this exercise, the sand volume fraction was estimated from well logs, assuming that lithofacies proportions at wells were representative of the entire reservoir area. A vertical proportion curve derived from the layer average of well data was calculated (fig. 10). The channel width, amplitude, wavelength and width-to-thickness values were assumed as in the constrained case. Three ranges of variability were considered to represent the uncertainty over channel directions (0°- 60°, 60°- 120°, 120°- 180°), with the minimum and maximum end members being 60° and 180° degree angles, respectively. One hundred unconstrained realizations were run for each of the three considered channel direction ranges. This number was verified to be statistically representative, as increasing the number of realizations did not materially change the results. An example of one of the 300 realizations of facies architecture generated by the MPS methodology as described above without any basin-scale constraints (fig. 11) is compared with a realization conditioned to the calculated vertical proportion curve (fig. 12), and with a realization conditioned to the 3D lithofacies probability distribution (fig. 13). Fig. 11 does not show any particular trend, neither horizontally (a) nor vertically (b). In fig. 12b the effect of the imposed vertical trend is clearly visible. In fig. 13 the effect of a 3D trend is clearly shown, both horizontally (a) and vertically (b).

In order to evaluate the local predictability obtainable without any basin constraining, the predicted sand probability (P_{sand}) was calculated from the 300 realizations described above, at the nine monitoring locations (W1-W9) shown in Fig. 5b. A sand probability curve for each location was calculated at each depth point as the ratio between the number of realizations exhibiting sand and the total number of reservoir realizations. The obtained curves were then compared with the imposed N/G value (arising from well data) and with the lithostratigraphy of the reference reservoir realization. In fig. 14a nine plots are displayed, one for each selected location (W1-W9) at which the reservoir scale lithological sequence has been monitored. The sand probability curve is distributed quite uniformly along the wells, according to the imposed sand fraction. In

other words, by averaging over a large number of realizations the mean N/G value of the reservoir is obtained almost uniformly everywhere. This is in accordance with the stationarity assumption. Because no information about channel trends was provided, the same statistical properties (mean N/G value) were assigned to the entire domain. Consequently, without information about the channel trends obtained from SFM, it is impossible to infer the channel architecture at the reservoir scale. Analogously, imposing a vertical proportion curve on the overall reservoir area would give a vertical predictability which is not representative of the entire reservoir. In particular, monitoring locations W1-W4 would be badly represented (cf. the vertical proportion curve in fig.10 and the W1-W4 stratigraphy in fig. 14).

In Figure 14b we show the average of 100 realizations which were generated with the 3D channel occurrence probability from the SFM simulation as an additional soft constraint. A significant vertical and horizontal variability of the sand probability curve is observed (fig. 14b), thus the channel location can actually be predicted. Furthermore channels and floodplain occurrence are statistically preserved, both locally as well as globally.

4.3 P_{CH} uncertainty propagated to the reservoir scale

Finally, the impact of inaccurate basin characterization on the quality of lithology prediction was investigated, by exploring the ranges of SFM input parameters. The uncertainty associated with the definition of the initial topography was represented by a set of 22 realizations, which were stochastically generated by perturbing the initial topographic surface of the reference case (Sacchi et al., 2015). The sediment entry point was located to the west side of the model, i.e. on the highest elevation of the surface dipping to the north east. Starting from an intermediate position on the west side, a range of 10 km to the north and to the south was considered. For the sea level, which was assumed to be constant during the simulated time interval, values in the range 35 to 60 m were considered, with a sampling interval of 0.5 meters. The definition of the highest sea level was based on well data. The main constraint on the lower boundary of sea level was the assumption that each well location (A, B, C, D) should be comprised of solely fluvial deposition, that is above sea level.

Following the approach of Sacchi et al. (2015), the uncertainty over basin parameters was propagated to P_{CH} and the possibility to reduce the resulting uncertainty by *a posteriori* check of the

scenario's goodness of fit was addressed. The results are shown in a depth-averaged 2D map (fig. 15a-15c) and in 1D vertical plot (fig.16a-16b), respectively. Figure 15a shows the P_{CH} values averaged over all the considered scenarios (2000); figure 15b provides the P_{CH} values averaged over a subset of the most likely scenarios (100) selected according to the F_{CH} and F_{top_surf} criteria (see Appendix) applied sequentially; figure 15c shows the P_{CH} values for the reference case. The P_{CH} variability in the vertical direction (fig. 16a and 16b) was evaluated for the specific locations W1-W9, displayed in fig. 5b. The P_{CH} median value over all considered scenarios (fig. 16a) and over the 100 most likely scenarios (fig. 16b) are compared to the reference case values. A clear improvement of the P_{CH} median was observed when we filtered out the scenarios that did not meet the goodness of fit criteria, especially at locations W3, W6 and W9. The comparison reveals how the selection of the most likely scenarios reduces the uncertainty related to the sandy channel occurrence at basin scale, which would be otherwise unfeasibly high (fig. 15a).

As already observed in a previous study (Sacchi et al., 2015), the goodness of fit trends observed for the considered reference case show significantly better values in the range of the sediment entry point 26-32 km and in the range of the sea level 40.5-50.5 m. As a consequence, the parameters were limited to those smaller ranges, thus reducing the number of scenarios considered for the analysis from thousands to hundreds. These scenarios were used to constrain the stochastic reservoir realizations, from which the sand probability distribution is estimated. The remaining uncertainty was propagated to the channel occurrence probability by SFM simulation, and subsequently to the reservoir 3D facies architecture following the Quasi-Monte Carlo approach. For each considered scenario 100 geostatistical realizations (MPS) were generated and the corresponding sand probability curves at W1-W9 locations were computed. Then, the sand probability uncertainty range was estimated at the W1-W9 monitoring locations based on the entire set of curves derived for the different scenarios. The uncertainty was expressed as the interval between the first and the third quartile of the corresponding distribution, which corresponds to the 25° and 75° percentile, respectively. Results are shown in figure 17. The black line represents the median of the local sand probability distribution obtained for all the considered scenarios, while the grey area represents the associated uncertainty (25°-75° percentile). On the right, the lithological stratigraphy of the reference case is shown. It can be noted that the presence of shale in the deeper layers is correctly detected, especially in wells

W5-W9. Conversely, the position of the sand intervals is subject to a high degree of uncertainty, especially in wells W1-W4. Thus, reliable SFM inference is essential for uncertainty reduction.

In order to investigate how efficiently the goodness of fit functions could be exploited to reduce the uncertainty at reservoir scale, the presented goodness of fit criteria (eq. A1-A2) were compared by extracting small subsets containing the most promising basin scenarios according to each criterion and calculating the corresponding uncertainty at reservoir scale. To make a fair comparison, instead of imposing thresholds on the goodness of fit values, subsets of equal size were extracted for each case: the 10 most promising basin scenarios according to each criterion were chosen, corresponding to 1000 reservoir realizations each.

Firstly, the goodness of fit based on the top stratigraphic surfaces (F_{top_surf}) was imposed in two variants: considering the entire basin area and restricting to the reservoir area only. In both cases the 10 most promising scenarios extracted had a sediment entry point between 28 and 30 km (reference case 30 km). However, only the goodness of fit calculated over the entire domain was able to identify the scenarios corresponding to the reference initial topography. Thus, the estimated sand probability distribution at reservoir scale was more precise and accurate when the entire domain was considered (fig. 18a vs fig. 18b). It is pointed out that the accuracy depends on the seismic resolution that was explicitly accounted for in equation A1 through a tolerance term.

Secondly, a subset of scenarios was extracted by comparing the stratigraphy at wells A, B, C, D with the corresponding channel occurrence probability at basin scale and selecting the 10 scenarios offering the best match in terms of F_{CH}. The uncertainty corresponding to this subset was very high (fig. 18c), which indicates that this criterion alone is not very informative, unless the number of available wells is large.

Finally, a combination of the two goodness of fit criteria (top stratigraphic surface at the basin scale and lithostratigraphy) was investigated. Different combinations of the two criteria were considered:

- **linear combination (F),** where each goodness of fit value was normalized by the mode of the corresponding distribution in order to weigh the two criteria. That is:

$$F = \frac{F_{CH}}{mode(F_{CH})} + \frac{F_{top\_surf}}{mode(F_{top\_surf})} \quad (4)$$

- **Pareto approach**: only the scenarios that had a set of goodness of fit values, which were not simultaneously improved by any other scenarios, were extracted.
- **Union** of the best five basin scenarios with respect to each criterion
- **Intersection** of the best scenarios from two bigger subsets; subsets of 100 scenarios for each criterion were necessary to find 10 intersections.
- **Cascade selection**: firstly the 30 most likely basin realizations with respect to their ability to fit the top stratigraphic surface were selected; among them, the 10 most likely realizations with respect to lithostratigraphy were extracted.

In the considered reference case, the union criterion gave the best results (fig. 18d).

5 DISCUSSION AND CONCLUSIONS

As shown in this study and Sacchi et al. (2015), reservoir modeling could significantly benefit from the integration of quantitative basin scale information obtained from SFMs. In particular, stratigraphic forward modelling can be used to steer the reconstruction of the internal reservoir geometry and to reduce the uncertainty in the distribution of the hydrocarbon-bearing lithologies. Uncertainty reduction is of crucial importance, especially during the early appraisal phase of a reservoir when relevant decisions have to be taken but few wells are drilled and, as a consequence, a limited amount of data is available to perform a reliable volumetric estimate. Furthermore, the prediction of the channel body geometry and stacking architecture in a fluvial depositional environment, can effectively assist in planning the strategy for new or infill wells.

The approach proposed in this paper has proved very efficient in estimating the lithological fraction of the hydrocarbon bearing rocks in a fluvio-deltaic environment. The integration of the basin information [i.e. the 3D channel-belt occurrence probability, the overall channel body (sand) versus floodplain (shale) volumes and the channel directions] was accomplished by geostatistical simulations. Two methodologies were considered, being the most widely used to describe channelized deposits: Object-Based Facies Modeling and

Multiple-Point Statistics. The latter offered a satisfactory integration of all the available information (i.e. reservoir and basin data), whereas the former proved to be less accurate.

The proposed workflow allows us to investigate the uncertainty affecting a reservoir model, arising from limited information on initial and boundary conditions of the basin-scale SFM, as well as from the adopted geostatistical approach for lithofacies simulation at the reservoir scale. An accurate assessment of initial and boundary conditions for the SFM is required for reliable prediction of channel locations and local to global N/G ratios. The reduction of the uncertainty of SFM input by application of a goodness of fit function significantly improved the predictability of the lithofacies distribution at reservoir scale. With the considered data set, the comparison between the SFM output with the stratigraphic surfaces derived from seismic interpretation proved to be extremely effective for inferring the SFM parameters. The effectivity is directly linked to the vertical and horizontal resolution and coverage of available seismic data. The effectivity of goodness of fit functions based on well lithology should increase with the number of wells. In exploration and appraisal phases when few wells are available, their effectivity is expected to be limited.

Significant improvement of the proposed methodology may be possible if the overall 3D reservoir architecture in the form of channel patterns can be evaluated rather than monitoring the lithology at defined reservoir locations as in the current analysis. In this way, the assessment of the uncertainty based on the sand probability from a joint distribution of the sand volumes rather than from a marginal distribution would be possible. Implementation of methods such as advocated by Karamitopoulos et al. (2014) would allow us to rigorously take into account the 3D relations of lithological bodies in the uncertainty estimation.

A careful calibration of SFMs was shown to be mandatory for uncertainty reduction. To this end the application of automatic search methods with the objective of finding a range of valid models will be investigated. A promising approach for this kind of application is a modification of the gradient-free neighborhood algorithm (Falivene et al., 2014). A logical next step is to apply the proposed methodology to a real-world case.

APPENDIX

The two goodness of fit functions used to filter the basin scenarios were presented in Sacchi et al. (2015) and are reported here for sake of completeness.

The function measuring the mismatch between evidence of channel /non-channel facies from a lithological log and the corresponding channel occurrence probability (P_{CH}) from simulated results was expressed by:

$$F_{CH} = \frac{1}{n_{wells}} \sum_{iw=1}^{n_{wells}} \left(\frac{1}{2} \left(\frac{1}{nz_{i_{iw}}} \sqrt{\sum_{z_i} \left(R_{iw}(z_i) = CH \right)^2} + \frac{1}{nz_{jiw}} \sqrt{\sum_{z_j} \left(R_{iw}(z_j) \neq CH \right)^2} \right) \right), where \;\; z_i \mid P_{CHiw}(z_i) = 0, \;\; z_j \mid P_{CHiw}(z_j) = 1 \tag{A1}$$

where $R_{iw}(z_i)$ is the lithology of well *iw* at the quote z_i, CH is the channel lithology, $P_{CH\,iw}(z_i)$ is the channel volume fraction of the grid cell intercepting the iw^{th} well at the depth z_i; nz_{iiw} is the number of depth points of the iw^{th} well that are expected for sure not to intercept a channel $\left(P_{CH\,iw}(z_i) = 0\right)$, analogously nz_{jiw} is the number of depth points of the iw^{th} well that are expected to surely intercept a channel $\left(P_{CH\,iw}(z_j) = 1\right)$; n_{wells} is the number of wells

The function expressing the goodness of fit with top seismic surface was defined as:

$$F_{top\_surf} = \frac{1}{\sqrt{n_x n_y}\sqrt{\sigma^2\left(z_{top\_surf}\right)}} \sqrt{\sum_{i,j} d\left(x_i, y_i\right)^2} \tag{A2}$$

where $n_x n_y$ is the number of cells of the grid covering the area; $\sigma^2\left(z_{top\_surf}\right)$ is the variance among depth data of the top surface and $d\left(x_i, y_i\right)$ is the punctual distance between surfaces, computed as:

$$d\left(x_i, y_i\right) = Max\left(\left| z_{top\_surf}(x_i, y_i) - z_{ref\_surf}(x_i, y_i) \right| - toll, 0\right) \tag{A3}$$

where $z_{top\_surf}\left(x_i, y_i\right)$ is the elevation of the simulated final topography in the cell corresponding to the coordinates x_i, y_i, $z_{ref\_surf}\left(x_i, y_i\right)$ is the elevation of the final topography in the same location according to seismic data and *toll* is a tolerance interval (i.e. 5m).

It should be pointed out that differently from hard data (i.e. well logs and well tops), seismic data is affected by a substantial degree of uncertainty. In fact, depth (geo)referencing of well logs is directly achieved by measuring the wire length at each acquisition point while depth (geo)referencing of seismic interpretation is obtained indirectly, and errors can occur in the interpretation phases (i.e. depth conversion of time data through the definition of a velocity model). Thus in the case of seismic data, the defined goodness of fit function accounts for a uncertainty in the reference data by considering zero misfit if the surface is comprised in a confidence interval of ± 5m for the seismic top surface horizon.

NOMENCLATURE

d = punctual distance between surfaces [m]

f = channel width to thickness ratio [-]

F_{CH} = fitness function evaluating misfit between P_{CH} and lithological log data[-]

F_{top_surf} = fitness function evaluating misfit between simulated top surface and seismic data [-]

h = channel thickness [m]

l_{CH} = channel length [m]

P_{CH} = channel occurrence probability [-]

P_{sand} = sand probability [-]

R = lithological log [-]

V_{cell} = grid cell volume [m^3]

V_{CH} = channel volume within a grid cell [m^3]

z_{ref_surf} = punctual elevation of reference top surface [m]

z_{top_surf} = punctual elevation of simulated top surface [m]

σ^2 = elevation variance [m^2]

REFERENCES

BENETATOS C. AND VIBERTI D., (2010). Fully Integrated Hydrocarbon Reservoir Studies: Myth or Reality? American Journal of Applied Sciences, Science Publications, 7(11): 1477-1486, doi: 10.3844/ajassp.2010.1477.1486.

BEUCHER, H., FOURNIER, F., DOLIGEZ, B., AND ROZANSKI, J. (1999). USING 3D SEISMIC-DERIVED INFORMATION IN LITHOFACIES SIMULATIONS. A CASE STUDY. Society of Petroleum Engineers. SPE Annual Technical Conference and Exhibition, 3-6 October, Houston, Texas. doi:10.2118/56736-MS.

CAERS J. AND ZHANG T., (2004). Multiple-point geostatistics: a quantitative vehicle for integrating geologic analogs into multiple reservoir models. AAPG Memoir Vol.80. pp. 383-394.

CAERS J., (2005). *Petroleum Geostatistics*. Society of Petroleum Engineers Inc. ISBN:978-1-55563-106-2.

CAFLISCH R. E., (1998). Monte Carlo and quasi-Monte Carlo methods, Acta Numerica, pp. 1-49, Cambridge University Press.

COCHRAN W. G., (1963). *Sampling Techniques*. Wiley Publications in statistics. John Wiley and Sons Inc, New York.

COSENTINO L., (2001). *Integrated Reservoir Studies*. Editions Technip., ISBN: 2-7108-0797-1.

DALMAN, R. A. F., WELTJE, G. J., (2008). Sub-grid parameterisation of fluvio-deltaic processes and architecture in a basin-scale stratigraphic model, Computers and Geosciences, Vol. 34 (10), pp. 1370–1380. doi:10.1016/j.cageo.2008.02.005

DALMAN, R. A. F., WELTJE, G. J., (2011). SimClast: An aggregated forward stratigraphic model of continental shelves, Computers and Geosciences, Vol. 38 (1), pp. 115-126. doi:10.1016/j.cageo.2011.05.014.

DALY, C. AND CAERS, J., (2010). Multi-point geostatistics – an introductory overview, First Break, Vol 28 (9), pp. 39-47, EAGE. doi: 10.3997/1365-2397.2010020.

DEUTSCH C.V. (2002). *Geostatistical Reservoir Modeling*. Oxford university press. ISBN: 0195138066.

FALIVENE O., FRASCATI A., GESBERT S., PICKENS J., HSU Y.,AND ROVIRA A., (2014) Automatic Calibration of Stratigraphic Forward Models for Predicting Reservoir Presence in Exploration. AAPG Bulletin, V. 98, No. 9, 1811–1835. doi: 10.1306/02271413028

GEORGSEN F., EGELAND T., KNARUD R. AND MORE H. (1994) Conditional simulation of facies architecture in fluvial reservoirs. In: Armstrong M. and Dowd P.A. (eds.) *Geostatistical simulations. Proceedings of the Geostatistical Simulation Workshop*, Fontainebleau, France, 27–28 May 1993, pp.235-250, Kluwer Academic Publishers, Dordrecht. ISBN 978-94-015-8267-4

GIBLING M. R., (2006). Width and thickness of fluvial channel bodies and valley fills in the geological record: a literature compilation and classification, Journal of Sedimentary Research, Vol. 76 (5), pp. 731-770. doi: 10.2110/jsr.2006.060.

HAUGE R. HOLDEN L., SYVERSVEEN A. R. (2007). Well Conditioning in Object Models, Mathematical Geology, Vol 39, pp. 383–398. doi 10.1007/s11004-007-9102-z.

HOWELL J. A., MARTINIUS A. W. , GOOD T. R. (2014). The application of outcrop analogues in geological modelling: a review, present status and future outlook From: Martinius, A. W., Howell, J. A. and Good, T. R. (eds) 2014. Sediment-Body Geometry and Heterogeneity:Analogue Studies for Modelling the Subsurface. Geological Society, London, Special Publications, Vol 387, pp.1–25. , doi:10.1144/SP387.12.

ISAAKS E. H., SRIVASTAVA M. R., (1989). *An introduction to Applied Geostatistics*, Oxford University Press, Inc., New York. ISBN 0-19-505012-6.

JOHNSON R. A., WICHERN D. W., (2002). *Applied multivariate statistical analysis*. Prentice Hall. ISBN: 0130925535.

KARAMITOPOULOS, P., WELTJE, G.J., DALMAN, R.A.F. (2014) Allogenic controls on autogenic variability in fluvio-deltaic systems: inferences from analysis of synthetic stratigraphy. Basin Research, Vol. 26, 767–779, doi: 10.1111/bre.12065

LABOURDETTE R., HEGRE J, IMBERT P., AND INSALACO E. (2008) Reservoir-scale 3D sedimentary modelling: approaches to integrate sedimentology into a reservoir characterization workflow. Geological Society, London, Special Publications, Vol.309, pp.75-85, doi:10.1144/SP309.6

MALLET J-L, (2002), *Geomodeling*, Applied geostatistics series, Oxford University Press. ISBN-10: 0195144600.

MARION, D., INSALACO, E., ROWBOTHAM, P., LAMY, P., AND MICHEL, B. (2000). Constraining 3D Static Models To Seismic And Sedimentological Data: A Further Step Towards Reduction Of Uncertainties. Society of Petroleum Engineers. SPE European Petroleum Conference, 24-25 October, Paris, France doi:10.2118/65132-MS.

MASSONNAT, G. J. (1999). Breaking of a Paradigm: Geology Can Provide 3D Complex Probability Fields for Stochastic Facies Modelling. Society of Petroleum Engineers. SPE Annual Technical Conference and Exhibition, 3-6 October, Houston, Texas. doi:10.2118/56652-MS.

MENEVEAU, C., (2010), Turbulence: sub-grid-scale modeling. scholarpedia, Vol.5 (1): 9489 doi:10.4249/scholarpedia.9489.

OLIVER, D.S.(1994): Multiple Realizations of the Permeability Field from Well-Test Data, paper SPE 27970 presented at the 1994 U. of Tulsa Centennial Petroleum Engineering Symposium, Tulsa, 29–31 August. doi: 10.2118/27970-PA

PAL S. K. (1998), *Statistics for Geoscientists - Techniques and applications.* Concept Publishing Company Ltd., New Delhi. ISBN 10: 8170227127.

REYNOLDS A. D., (1999) Dimensions of Paralic Sandstone Bodies, AAPG Bulletin, Vol. 83 (2), pp. 211-229.

SACCHI Q., WELTJE G. J., VERGA F. (2015) Towards Process-Based Geological Reservoir Modelling: Obtaining Basin-Scale Constraints from Seismic and Well Data. Marine and Petroleum Geology. Elsevier. Vol. 61. pp. 56-68. doi: 10.1016/j.marpetgeo.2014.11.002

STREBELLE S. (2012) Multiple-Point Geostatistics: from Theory to Practice, Ninth International Geostatistics Congress, Oslo, Norway June 11 – 15, 2012.

STREBELLE, S., (2002): Conditional Simulation of Complex Geological Structures Using Multiple-Point Statistics. Mathematical Geology. VOL 34 Issue 1, pp 1-21. Kluwer Academic Publishers-Plenum Publishers. doi: 10.1023/A:1014009426274. ISSN 1573-8868

STREBELLE, S., PAYRAZYAN, K., AND CAERS, J. (2003). Modeling of a Deepwater Turbidite Reservoir Conditional to Seismic Data Using Principal Component Analysis and Multiple-Point Geostatistics. Society of Petroleum Engineers. doi:10.2118/85962-PA

SYVERSVEEN A. R., HAUGE R., TOLLEFSRUD J. I., LAEGREID U., MACDONALD A. (2011), A Stochastic Object Model Conditioned to High-Quality Seismic Data, Mathematical Geology, Vol. 43, pp. 763-781. doi: 10.1007/s11004-011-9355-4

TETZLAFF D., DAVIES R., MCCORMICK D., SIGNER C., MIROWSKI P., WILLIAMS N, HODGSON D., BRADY J., (2005) Application of multipoint geostatistics to honor multiple attribute constraints applied to a deepwater outcrop analog, Tanqua Karoo Basin, South Africa. SEG /Houston 2005 Annual Meeting, Houston, Texas, 6–11 November 2005.

VOSE D. (1996). *Quantitative Risk Analysis*. John Wiley and Sons, New York.

WEN, X.-H., DEUTSCH, C.V., AND CULLICK, A.S. (1998): High resolution reservoir models integrating multiple-well production data, SPE-52231-PA. SPE Journal. doi: 10.2118/52231-PA.

ZACHARIASSEN E. MEISINGSET H., OTTERLEI C. , ANDERSEN T., ,HATLAND K. , HOYE T., MANGEROY G. , LIESTOL F. (2006). Method for conditioning the reservoir model on 3D and 4D elastic inversion data applied to a fluvial Reservoir In The North Sea SPE Europec/EAGE Annual Conference and Exhibition, 12-15 June, Vienna, Austria. SPE-100190-MS. doi: 10.2118/100190-MS

FIGURE CAPTIONS

Fig. 1: Resolution and coverage of a typical data set for geological reservoir modeling.

Fig. 2: Geological reservoir modeling workflow proposed in this study.

Fig. 3: 3D view of basin-scale model in terms of net to gross and fluvial architecture at reservoir scale. Reference wells A to D are displayed. Comparison of gridding at basin and reservoir scale is shown (b).

Fig. 4: Lithology at wells A, B, C, D (reference case).

Fig. 5: (a) 3D channel occurrence probability distribution (reference case) at the basin scale in the reservoir area and (b) plane map showing wells (A, B, C, D) and monitoring locations (W1-W9); gridding at basin and reservoir scale is also displayed.

Fig. 6: Simulations with the geostatistical (a) object modeling and (b) multipoint geostatistics of the 3D fluvial architecture at the reservoir scale for the reference case (fig.5).

Fig. 7: Channel volume fraction at basin scale as obtained from volume-weighted upscaling of the reservoir realizations of fig. 8: (a) object modeling and (b) multipoint geostatistics.

Fig. 8: Maps of the depth-averaged error of volume-weighted upscaling of the 3D lithofacies distributions (fig. 9) with respect to the imposed 3D lithofacies distributions (fig.7): (a) object modeling and (b) multipoint geostatistics.

Figure 9: Channel occurrence probability curve (1D) at the basin scale (center) at wells W1, W3, W5, W7,W9 and corresponding stratigraphy obtained by multipoint geostatistics (right) and object modeling (left).

Fig. 10: Original lithofacies proportion (a) and sand probability curve (b) as derived from well data.

Fig. 11: Example of multipoint reservoir realization constrained to wells A, B, C, D with imposed average N/G computed from well data: (a) 3D view; (b) frontal section.

Fig. 12: Example of multipoint reservoir realization constrained to wells A, B, C, D with imposed vertical proportion curve computed from well data: (a) 3D view, (b) frontal section compared to imposed vertical proportion curve.

Fig. 13: Example of multipoint reservoir realization constrained to wells A, B, C, D with imposed 3D facies probability distribution arising from basin model: (a) 3D view, (b) frontal section (c) frontal section of facies probability distribution cube.

Fig. 14: Monitoring locations W1-W9: sand probability curves unconditioned (a) and conditioned (b) to the 3D channel occurrence probability distribution as calculated from a statistically representative number of reservoir realizations (MPS approach). Each plot comprises two columns. In the first column, the sand probability curve (black line) is plotted against the imposed N/G (red line) (a) or channel occurrence probability of the reference case (b). The second column represents the lithological sequence at reservoir scale for the base case scenario.

Fig. 15: Reduction of uncertainty over channel occurrence probability (P_{CH}) at basin scale: average over all scenarios (a), average over a subset of selected scenarios (b), reference case (c). P_{CH} values shown in 2D map corresponding to the reservoir area are depth-averaged.

Fig. 16: Reduction of uncertainty over channel occurrence probability (P_{CH}) at basin scale at selected monitoring locations (W1-W9): all scenarios (a) and 100/2000 most likely scenarios (b), where F_{CH} and F_{top_surf} criteria (see Appendix) were sequentially applied.

Fig. 17: Sand probability curves and their associated uncertainties, arising from uncertainty of the 3D channel occurrence probability, which in turn reflects the uncertainty of SFM parameters.

Fig. 18: Uncertainty reduction via selection of SFM realizations by goodness of fit evaluation; comparison of different goodness of fit functions: (a) top stratigraphic surface fitting in the basin area; (b) top stratigraphic surface fitting in the reservoir area; (c) lithostratigraphy fitting at wells A, B, C, D; (d) union of the best five basin scenarios with respect to criterion of (a) and (c).

Figure 1

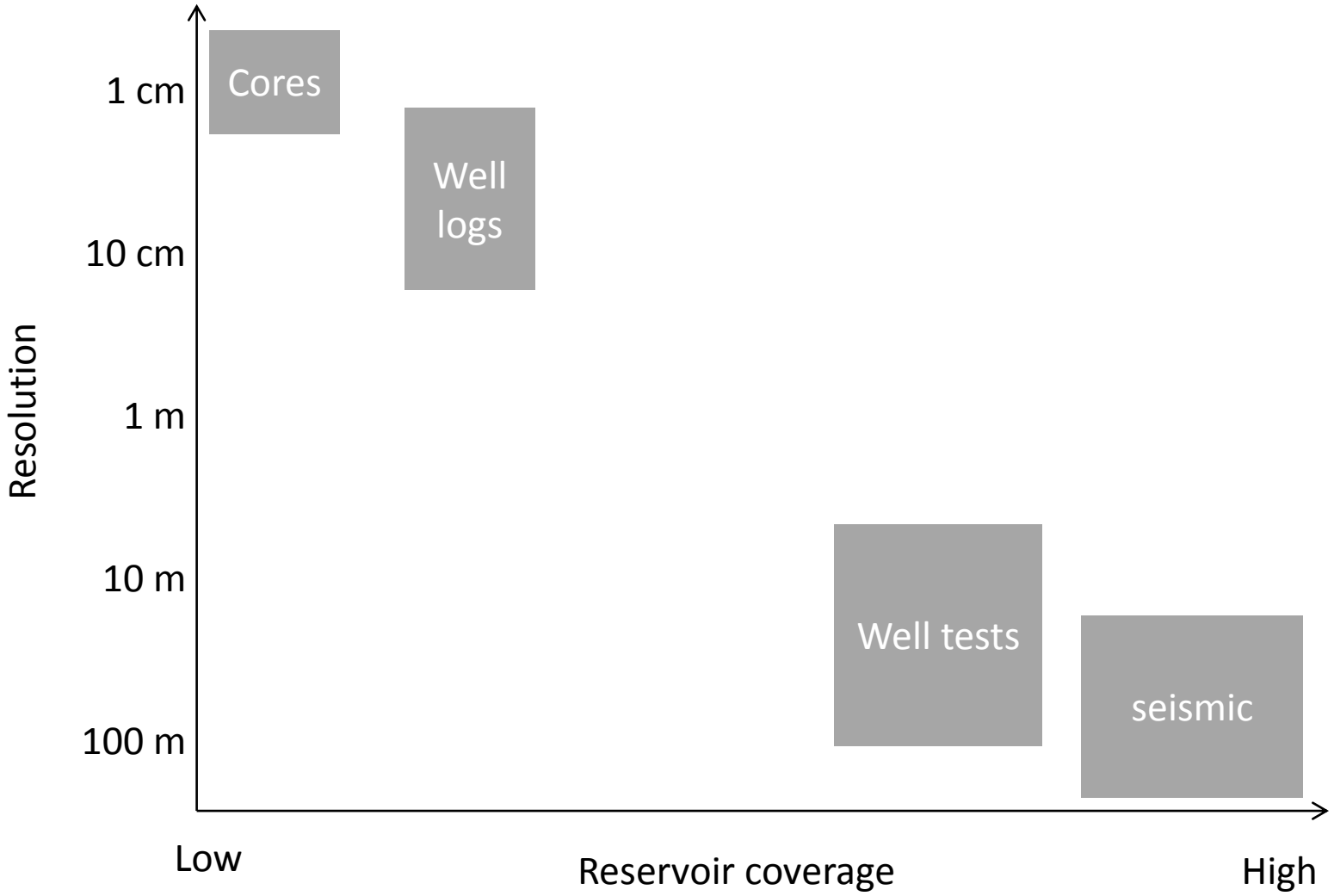
Cores
Well logs
Well tests
seismic
1 cm
10 cm
1 m
10 m
100 m
Resolution
Low
Reservoir coverage
High

Figure 2

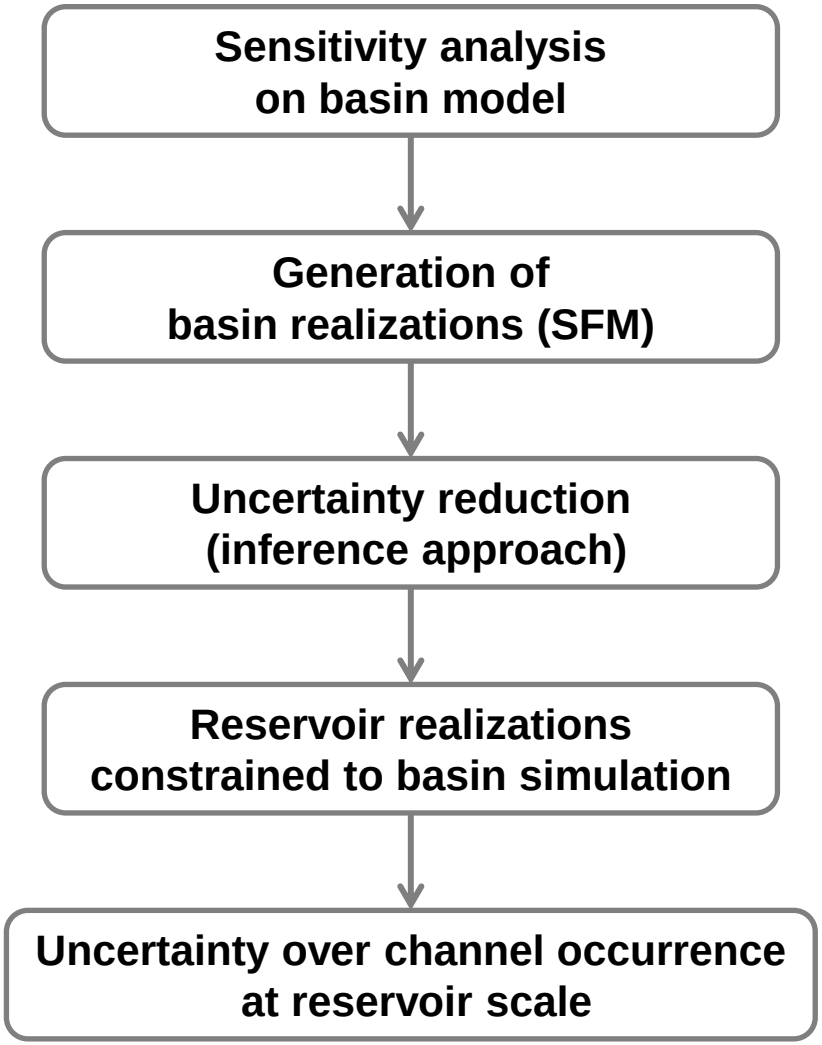
Sensitivity analysis
on basin model
Generation of
basin realizations (SFM)
Uncertainty reduction
(inference approach)
Reservoir realizations
constrained to basin simulation
Uncertainty over channel occurrence
at reservoir scale

Figure 3

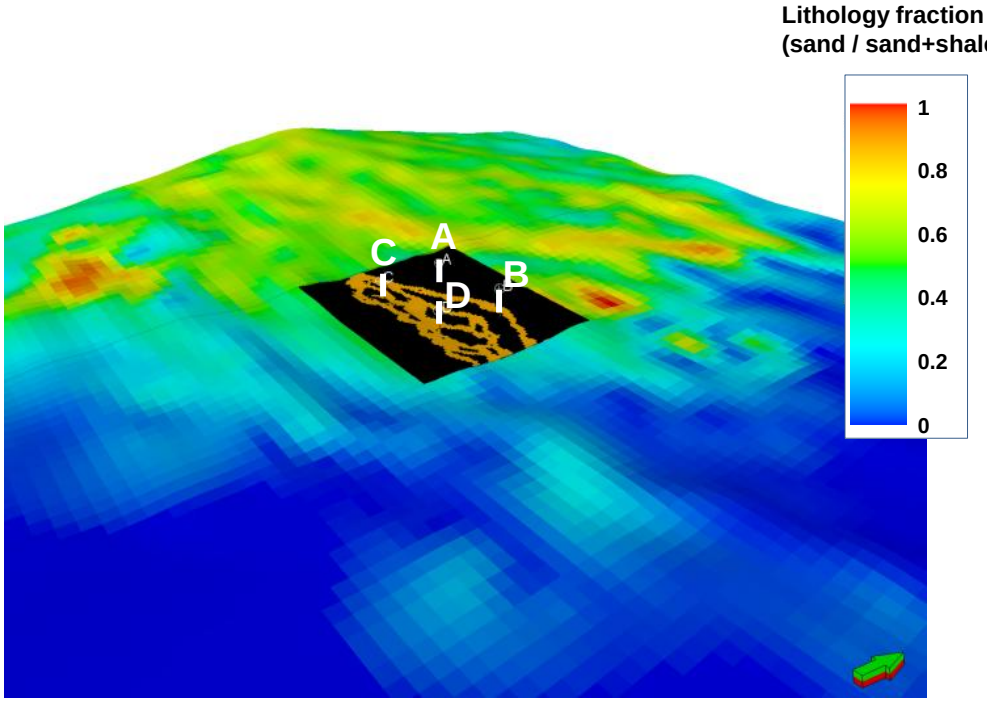

(a)

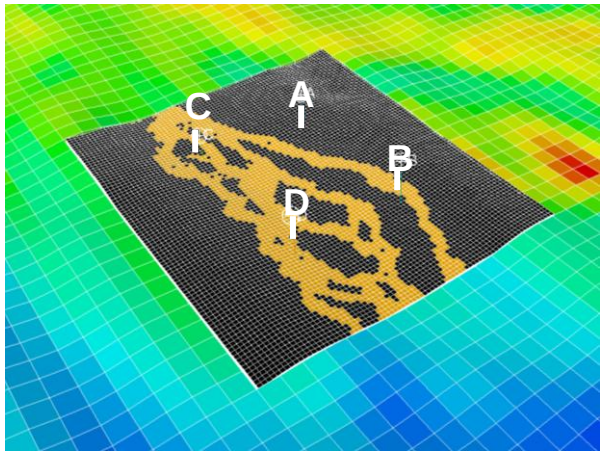

Basin cell size = 1x1 km
Reservoir cell size =100 x100 m

(b)

Figure 4

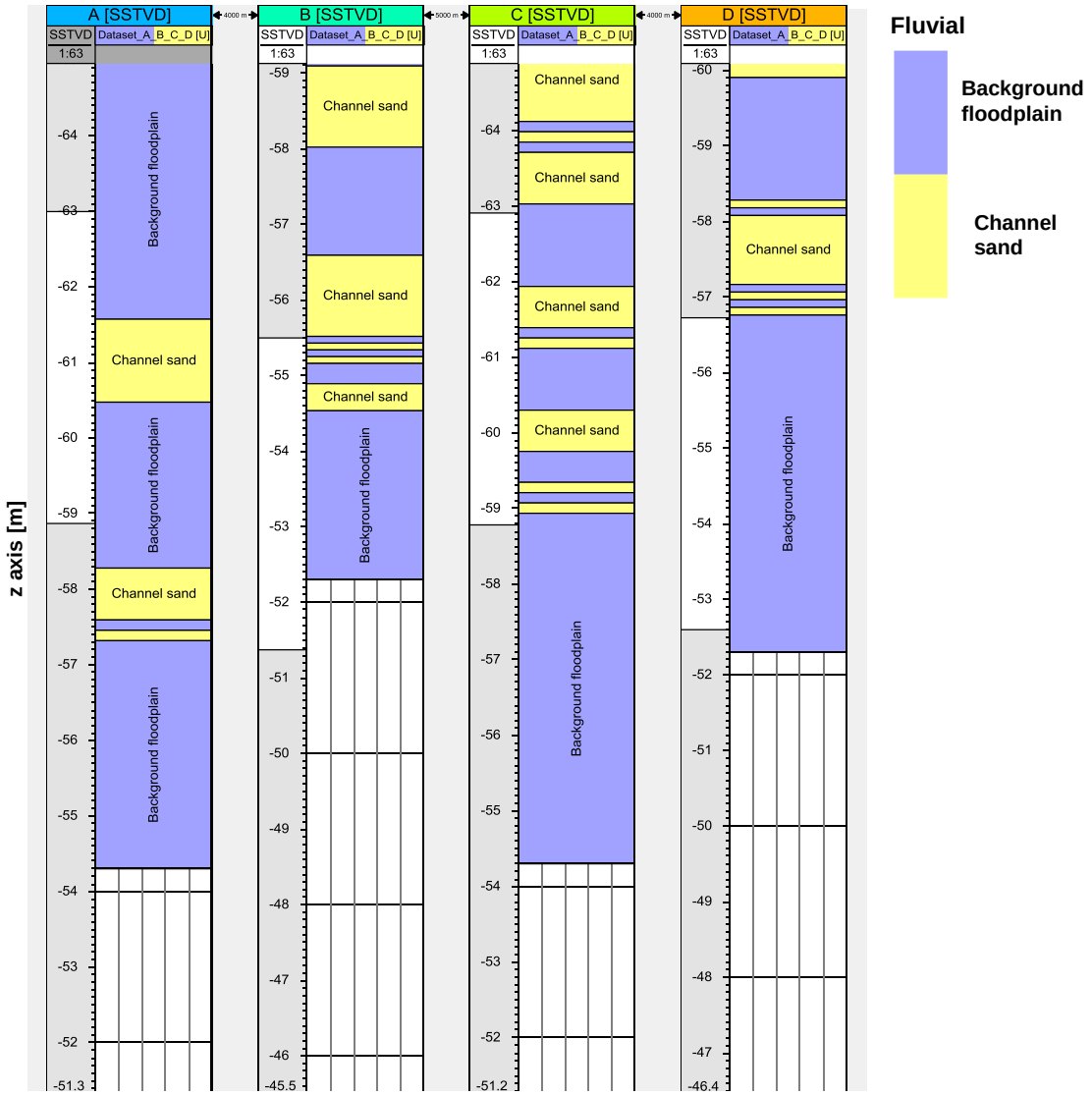
A [SSTVD]
B [SSTVD]
C [SSTVD]
D [SSTVD]
SSTVD
Dataset_A_B_C_D [U]
1:63
4000 m
5000 m
z axis [m]
Background floodplain
Channel sand
Fluvial
Background floodplain
Channel sand

Figure 5

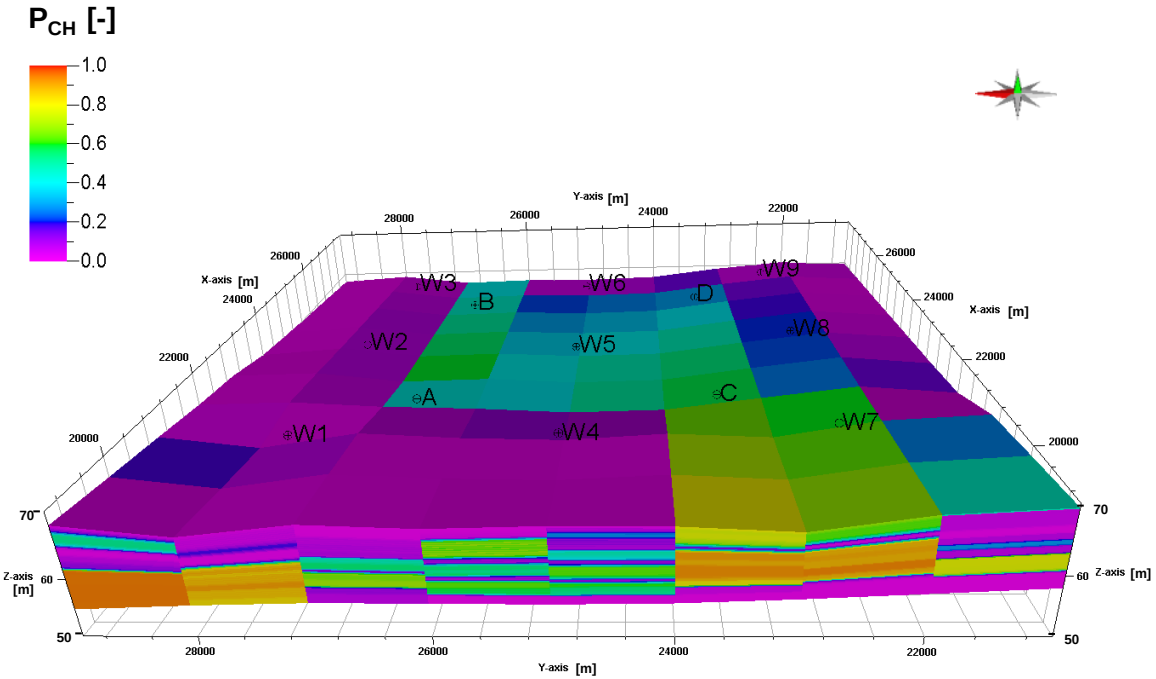
P_{CH} [-]
1.0
0.8
0.6
0.4
0.2
0.0
Y-axis [m]
X-axis [m]
Z-axis [m]
W1
W2
W3
W4
W5
W6
W7
W8
W9
A
B
C
D

(a)

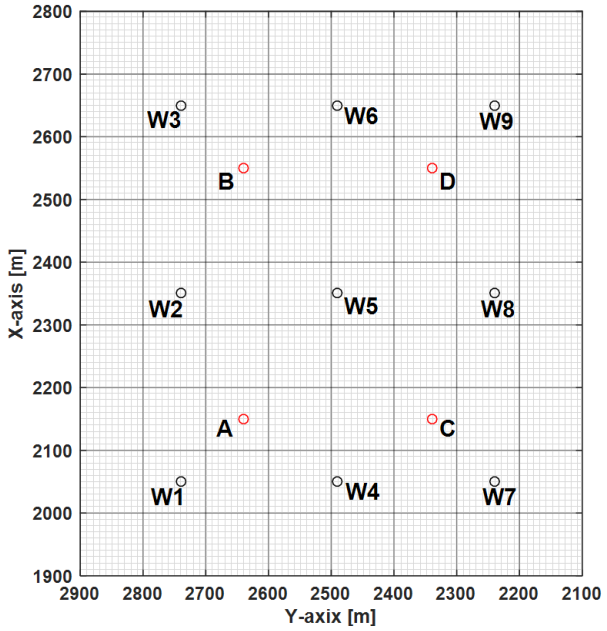
X-axis [m]
Y-axix [m]
W1
W2
W3
W4
W5
W6
W7
W8
W9
A
B
C
D

(b)

Figure 6

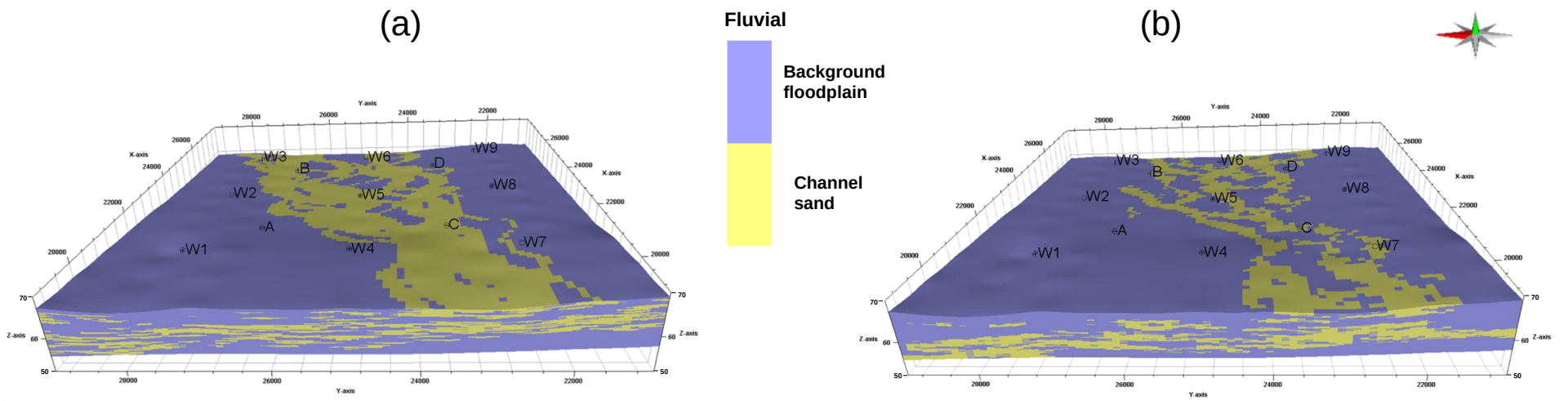
(a)
Fluvial
Background floodplain
Channel sand
(b)
W1
W2
W3
W4
W5
W6
W7
W8
W9
A
B
C
D
X-axis
Y-axis
Z-axis

Figure 7

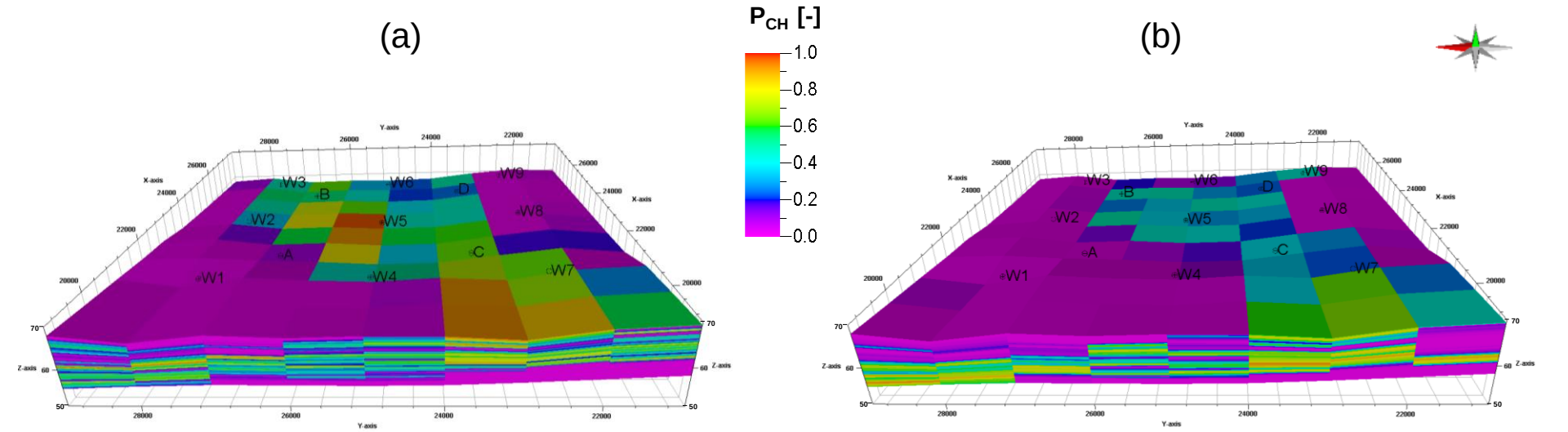
(a)
P_{CH} [-]
1.0
0.8
0.6
0.4
0.2
0.0
(b)
W1
W2
W3
W4
W5
W6
W7
W8
W9
A
B
C
D
X-axis
Y-axis
Z-axis

Figure 8

(a)

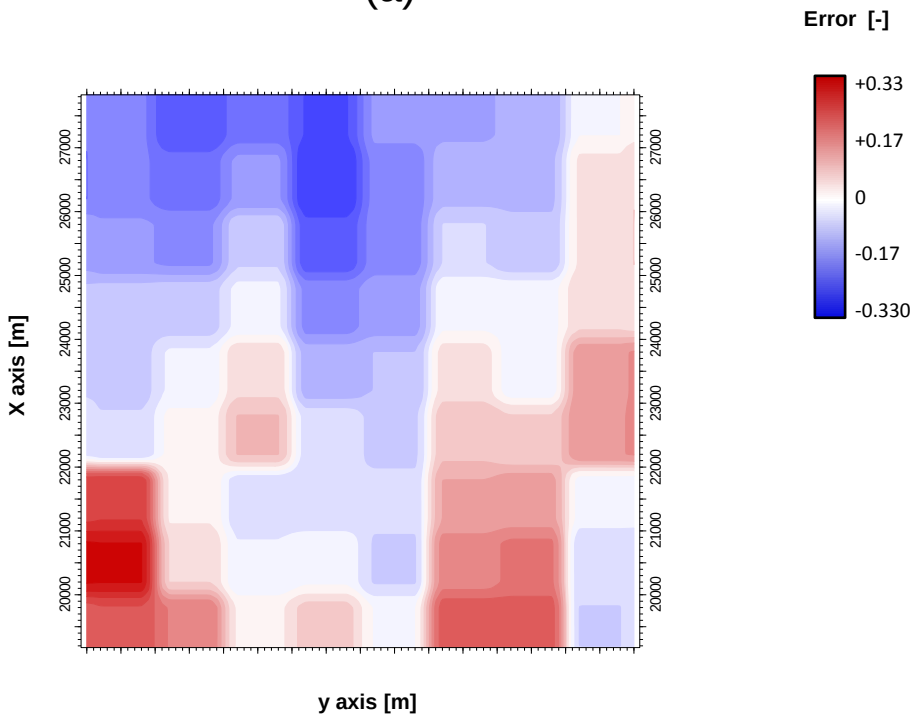

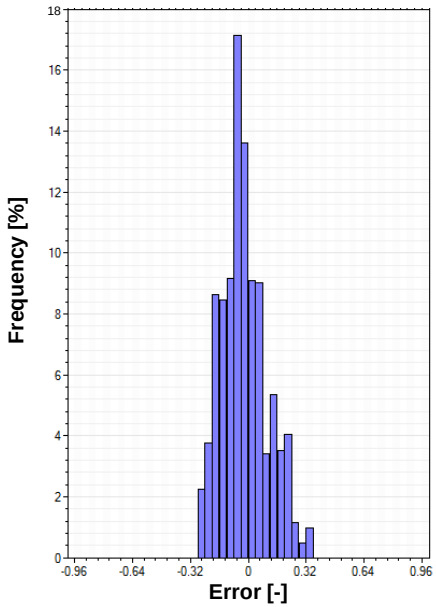

Min:	-0.26913
Max:	0.33352
Mean:	-0.02186
Std. dev.	0.12671

(b)

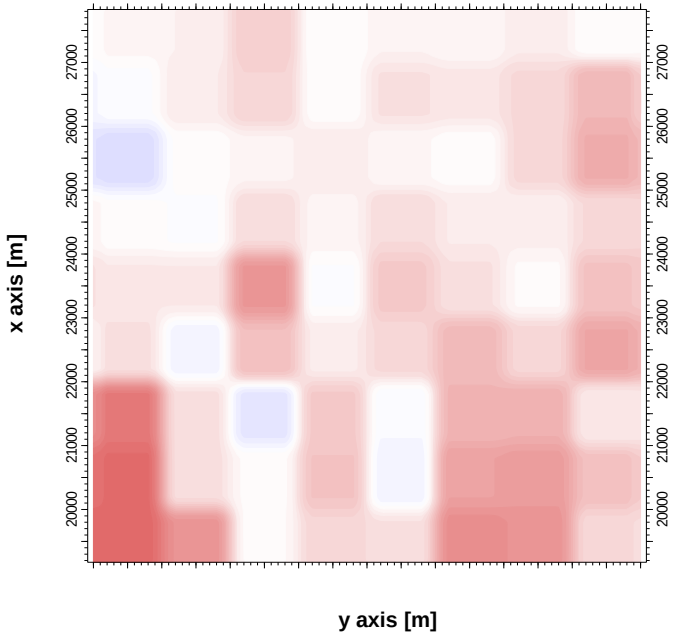

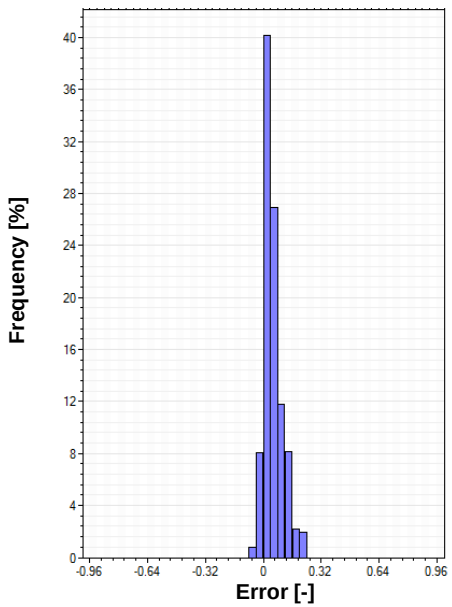

Min:	-0.04653
Max:	0.20885
Mean:	0.05200
Std. dev.	0.05143

Figure 9

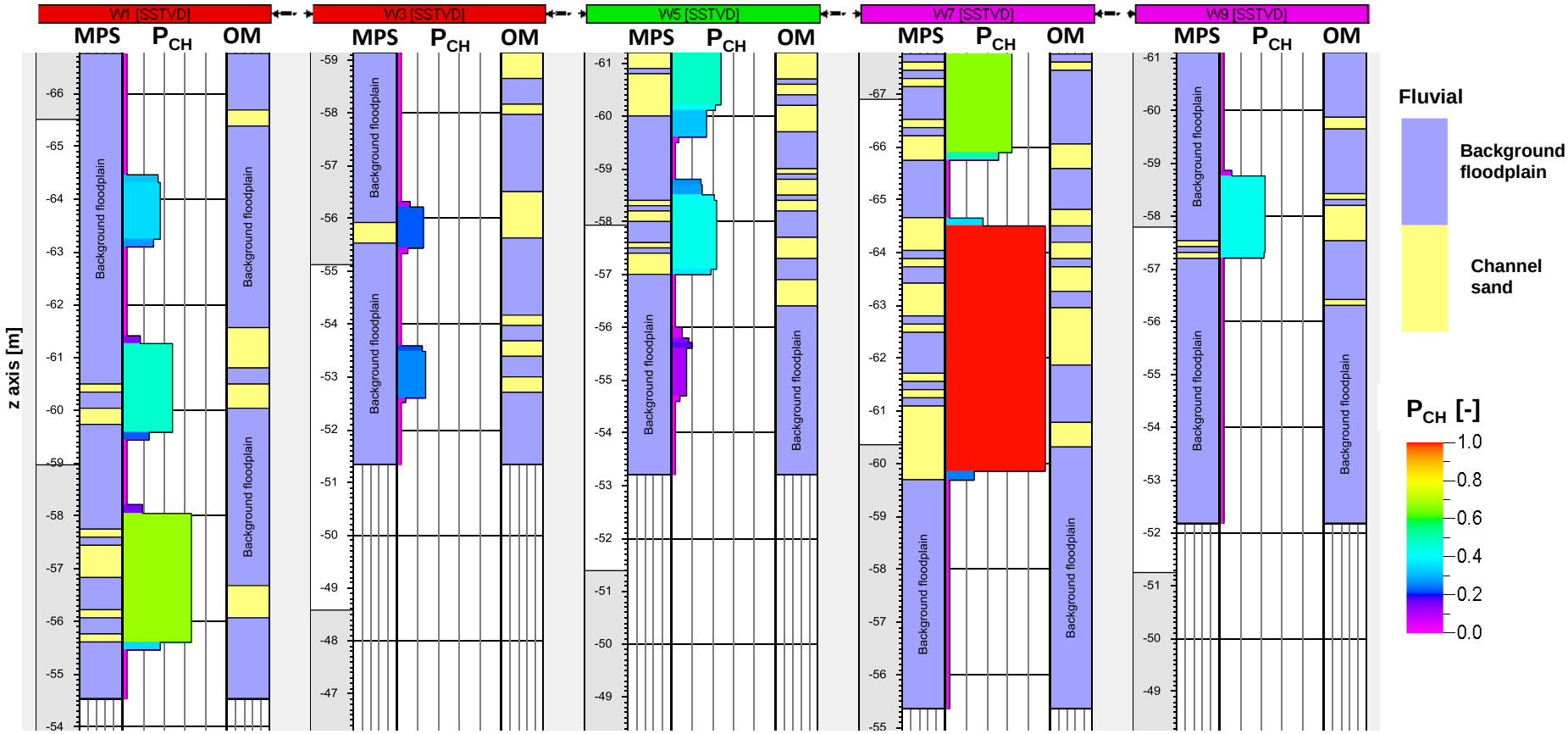
W1 [SSTVD]
W3 [SSTVD]
W5 [SSTVD]
W7 [SSTVD]
W9 [SSTVD]
MPS
P_CH
OM
z axis [m]
Background floodplain
Channel sand
Fluvial
P_CH [-]
1.0
0.8
0.6
0.4
0.2
0.0

Figure 10

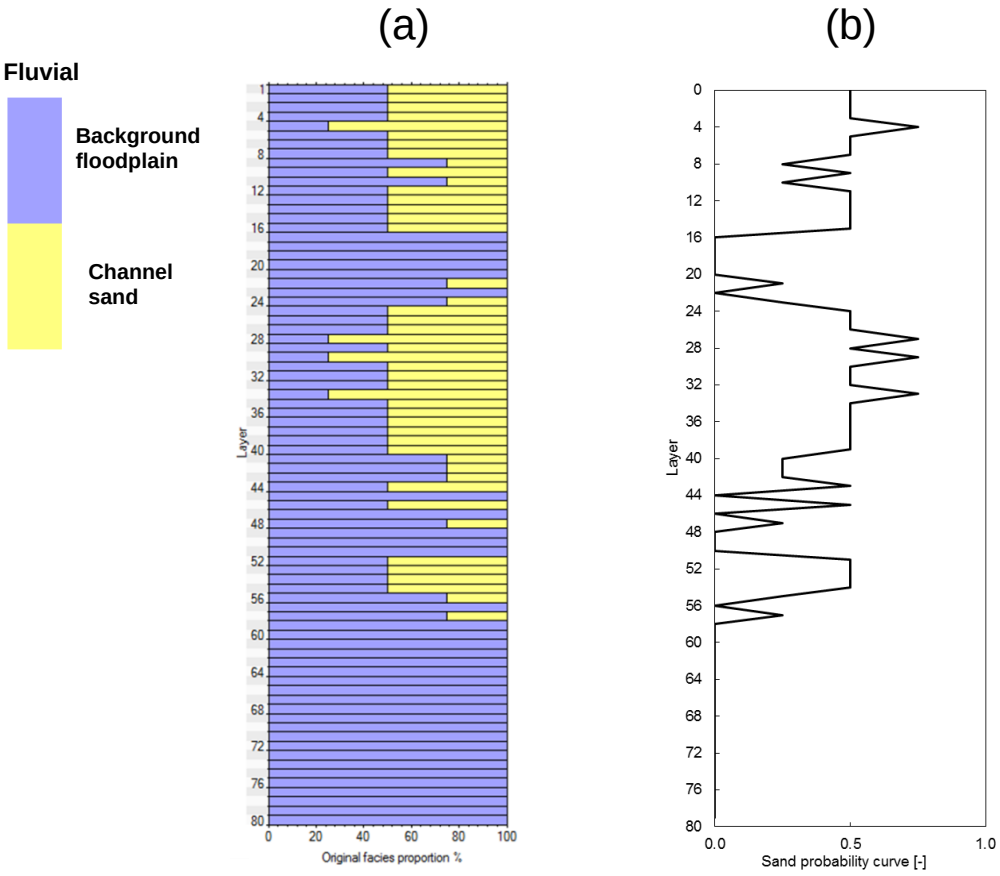
(a)
(b)
Fluvial
Background floodplain
Channel sand
Layer
Original facies proportion %
Sand probability curve [-]

Figure 11

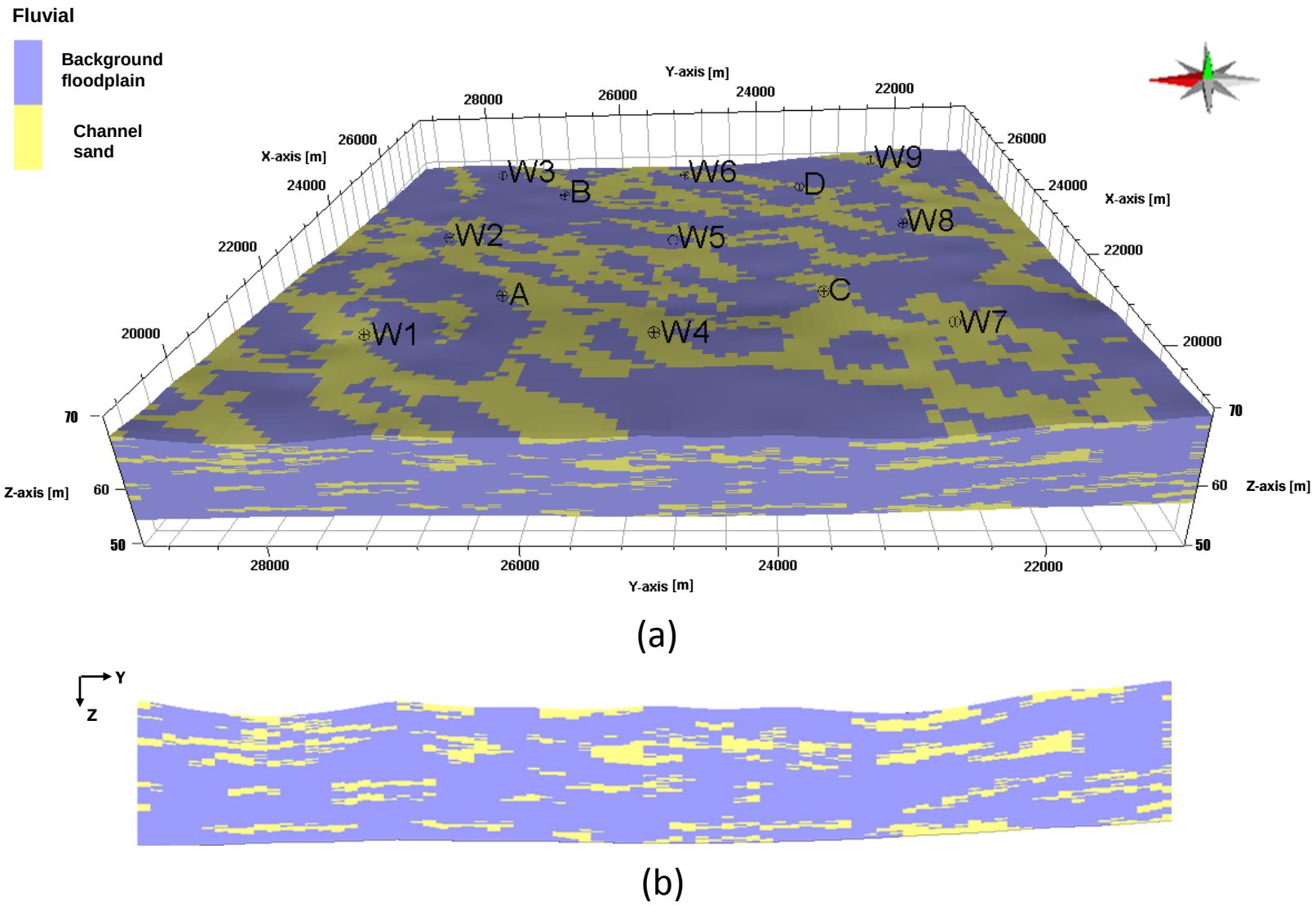
Fluvial
Background floodplain
Channel sand
Y-axis [m]
28000
26000
24000
22000
X-axis [m]
26000
24000
22000
20000
70
60
50
Z-axis [m]
W1
W2
W3
W4
W5
W6
W7
W8
W9
A
B
C
D
(a)
Y
Z
(b)

Figure 12

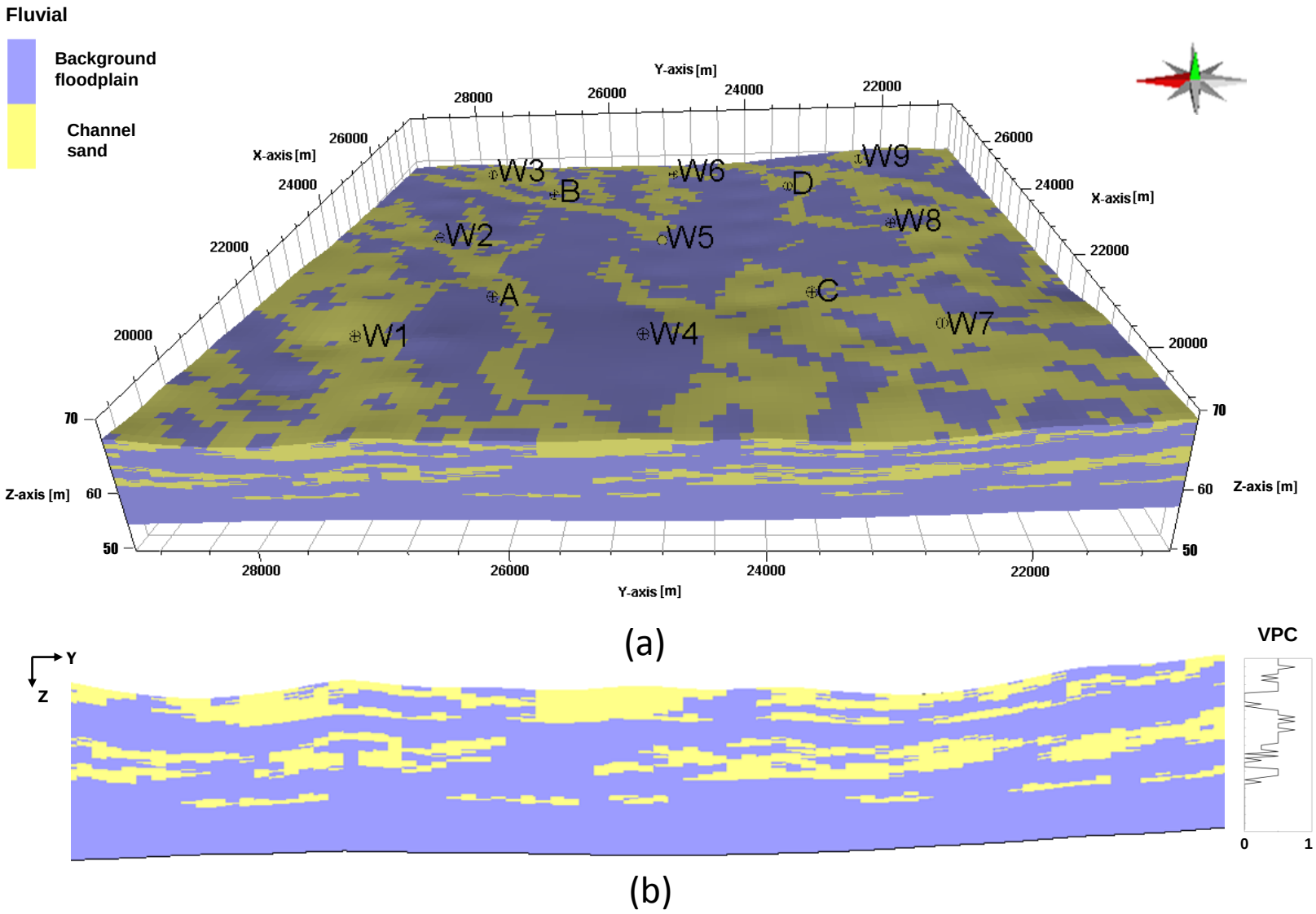
Fluvial
Background floodplain
Channel sand
Y-axis [m]
28000
26000
24000
22000
X-axis [m]
26000
24000
22000
20000
70
60
50
Z-axis [m]
W1
W2
W3
W4
W5
W6
W7
W8
W9
A
B
C
D
(a)
Y
Z
VPC
0
1
(b)

Figure 13

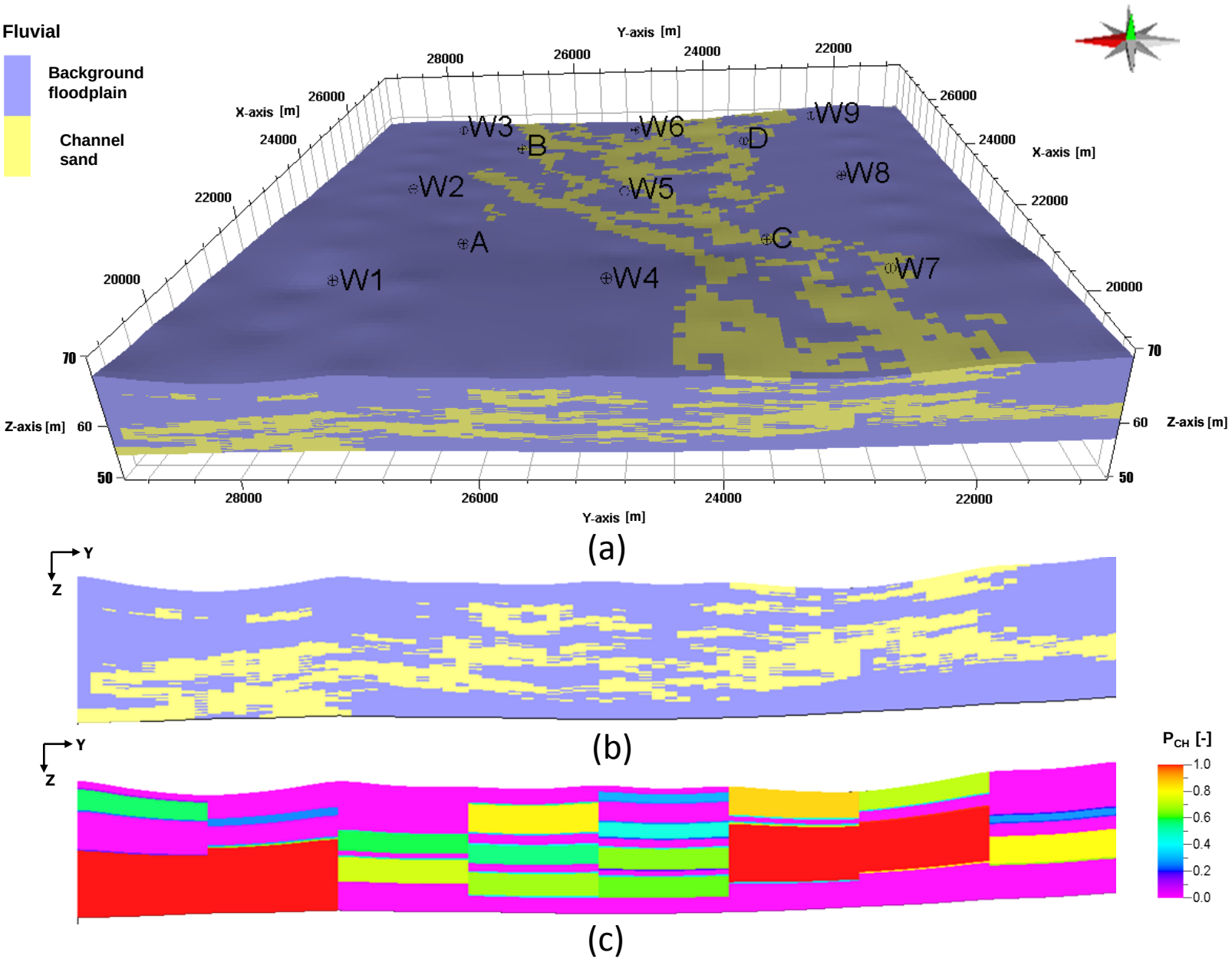
Fluvial
Background floodplain
Channel sand
Y-axis [m]
28000
26000
24000
22000
X-axis [m]
26000
24000
22000
20000
W1
W2
W3
W4
W5
W6
W7
W8
W9
A
B
C
D
70
60
50
Z-axis [m]
(a)
Y
Z
(b)
(c)
P_{CH} [-]
1.0
0.8
0.6
0.4
0.2
0.0

Figure 14

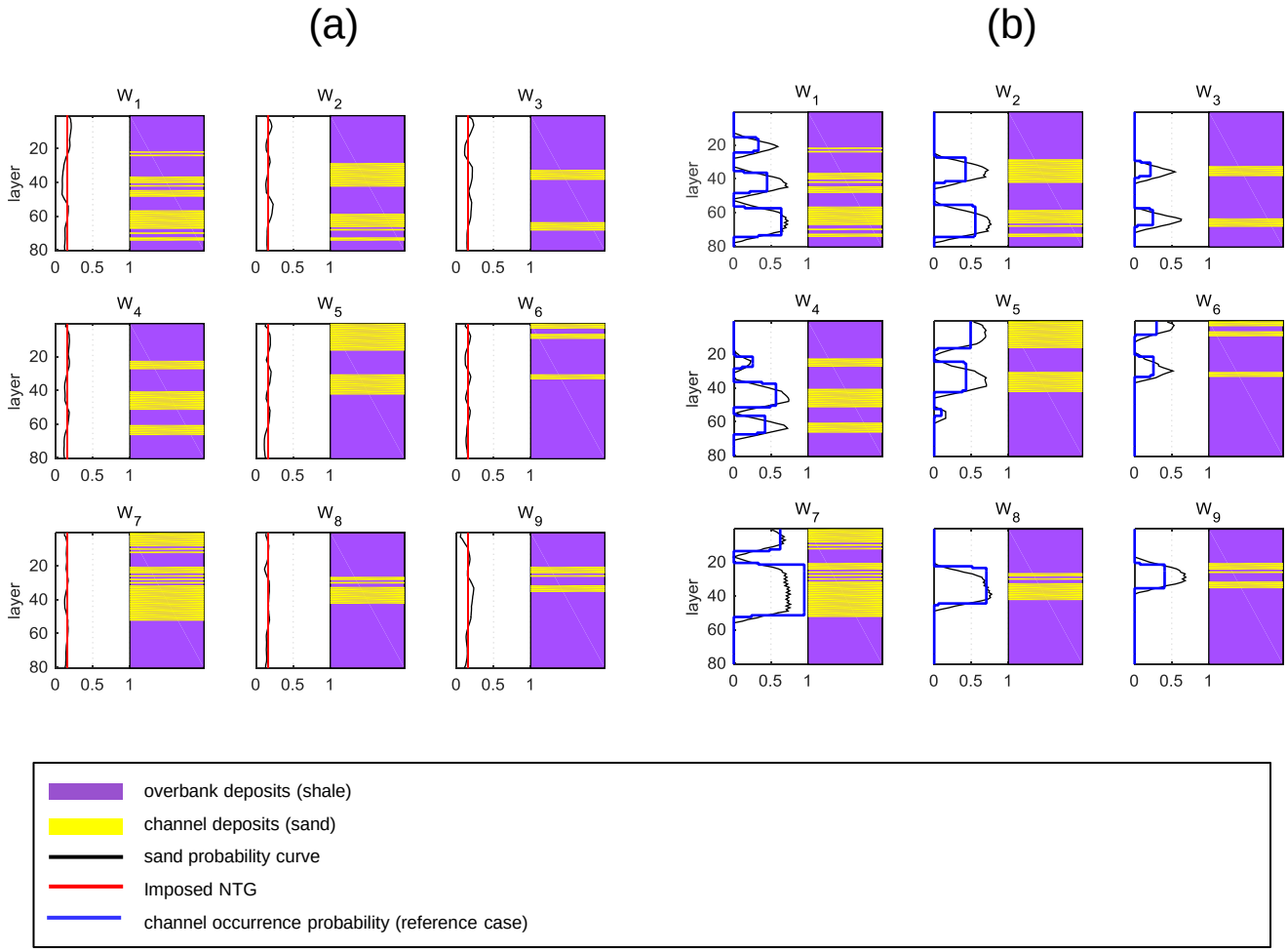
(a)
(b)
W1
W2
W3
W4
W5
W6
W7
W8
W9
layer
20
40
60
80
0
0.5
1
overbank deposits (shale)
channel deposits (sand)
sand probability curve
Imposed NTG
channel occurrence probability (reference case)

Figure 15

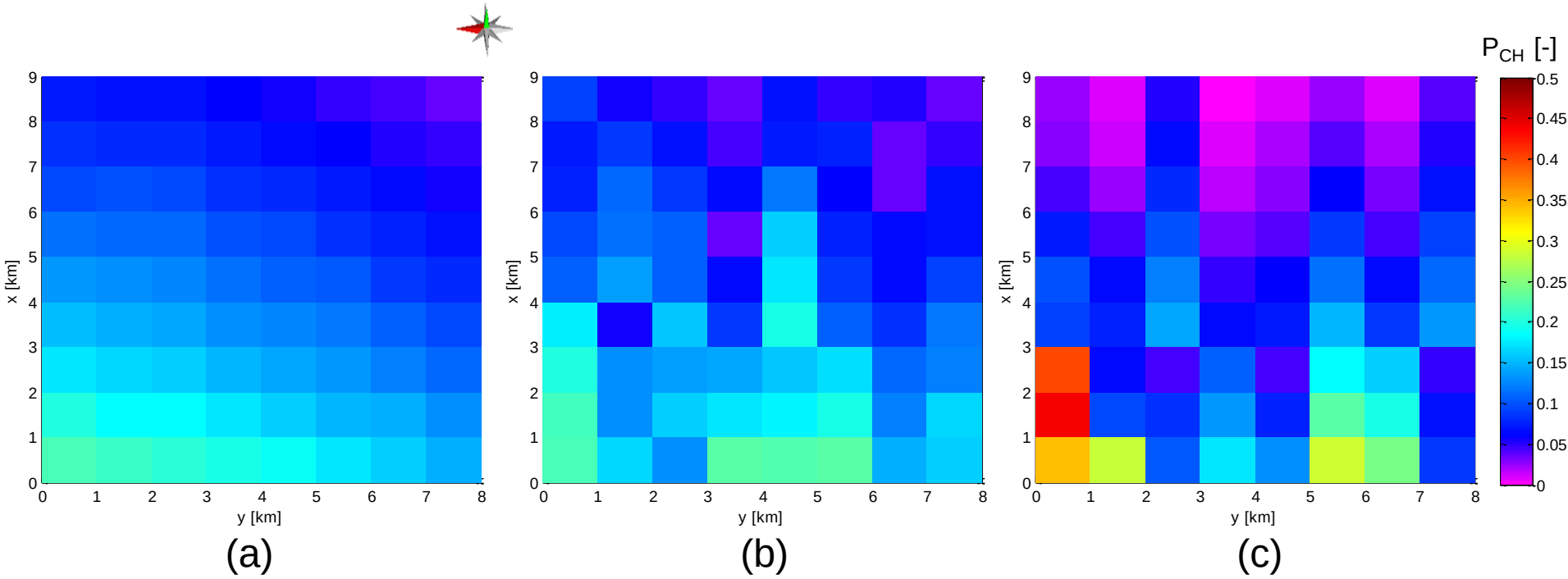

Figure 16

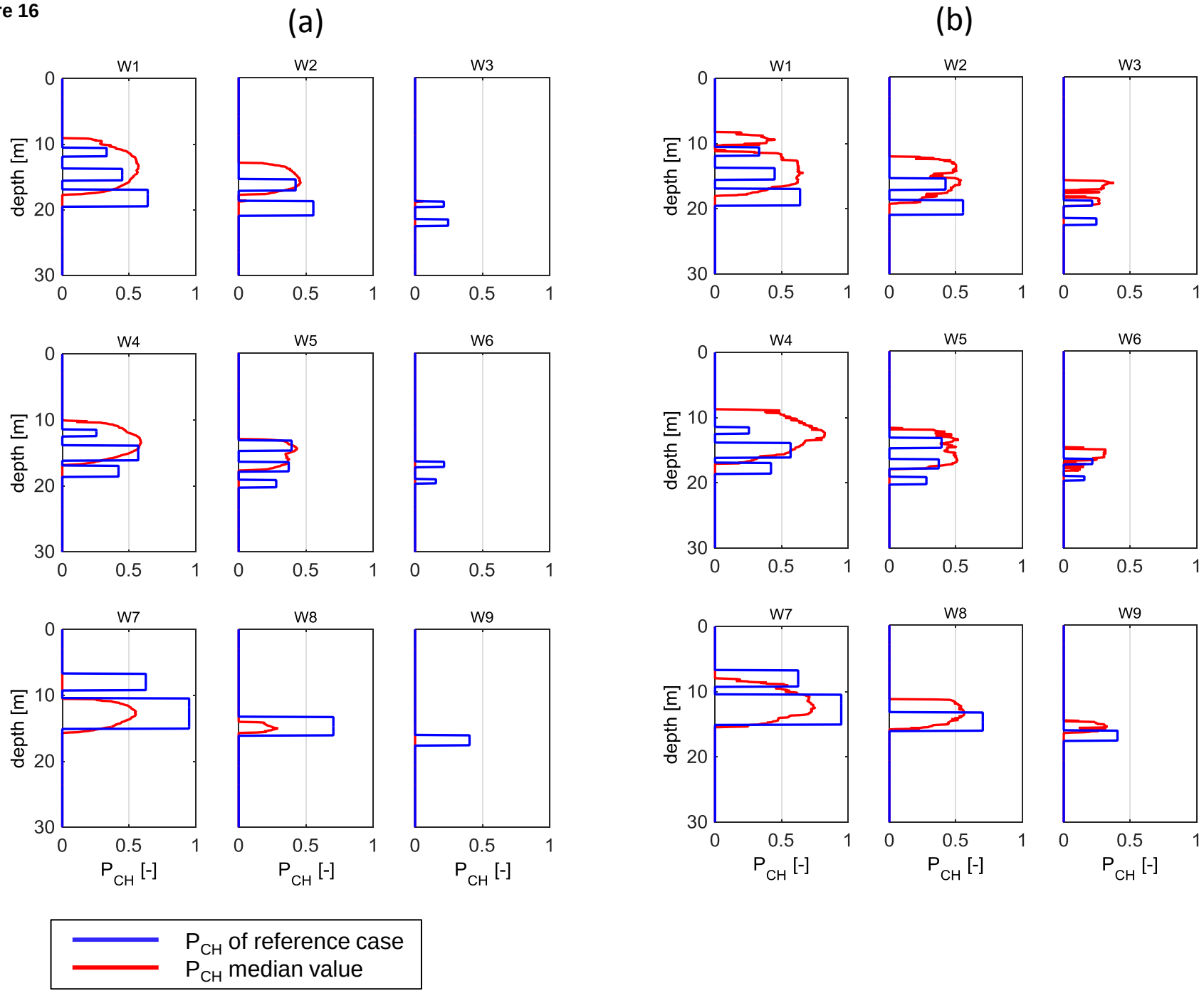
(a)
(b)
W1
W2
W3
W4
W5
W6
W7
W8
W9
depth [m]
0
10
20
30
0
0.5
1
P CH [-]
P CH of reference case
P CH median value

Figure 17

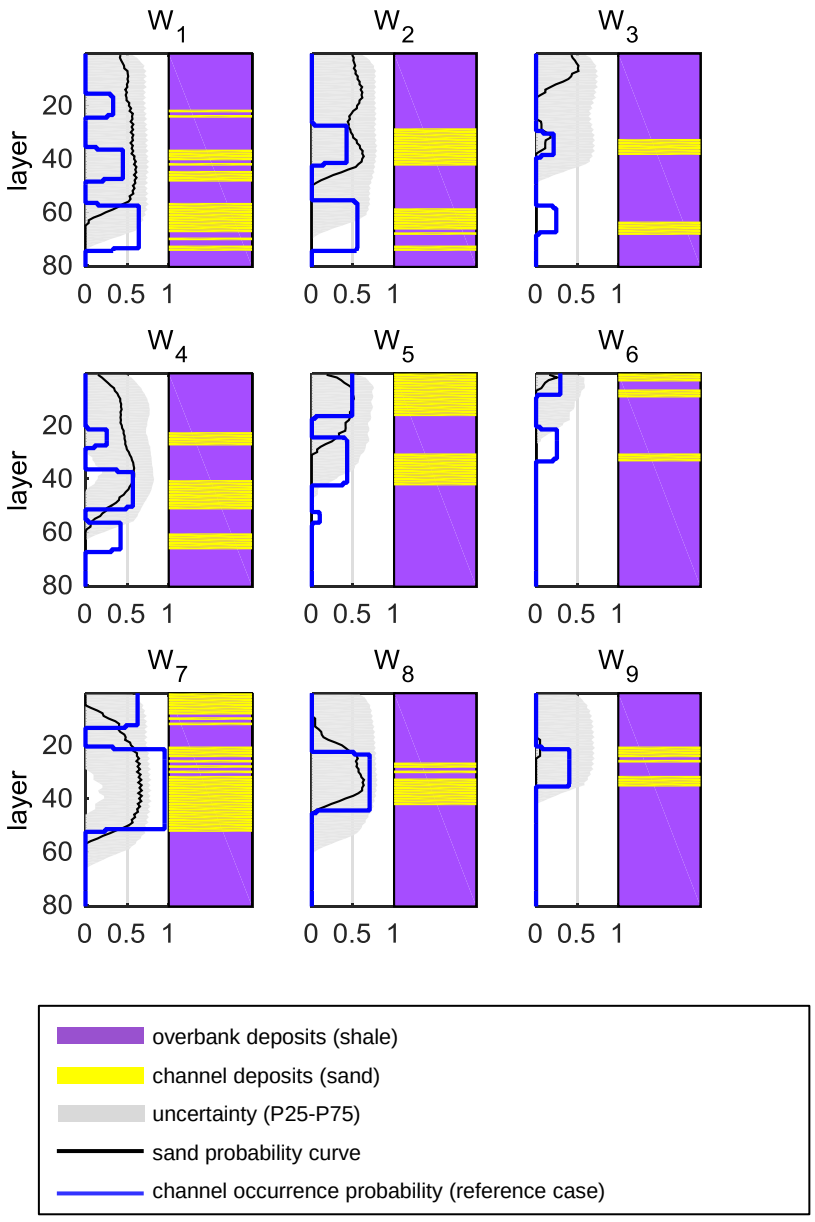
W1
W2
W3
W4
W5
W6
W7
W8
W9
layer
20
40
60
80
0 0.5 1
overbank deposits (shale)
channel deposits (sand)
uncertainty (P25-P75)
sand probability curve
channel occurrence probability (reference case)

Figure 18

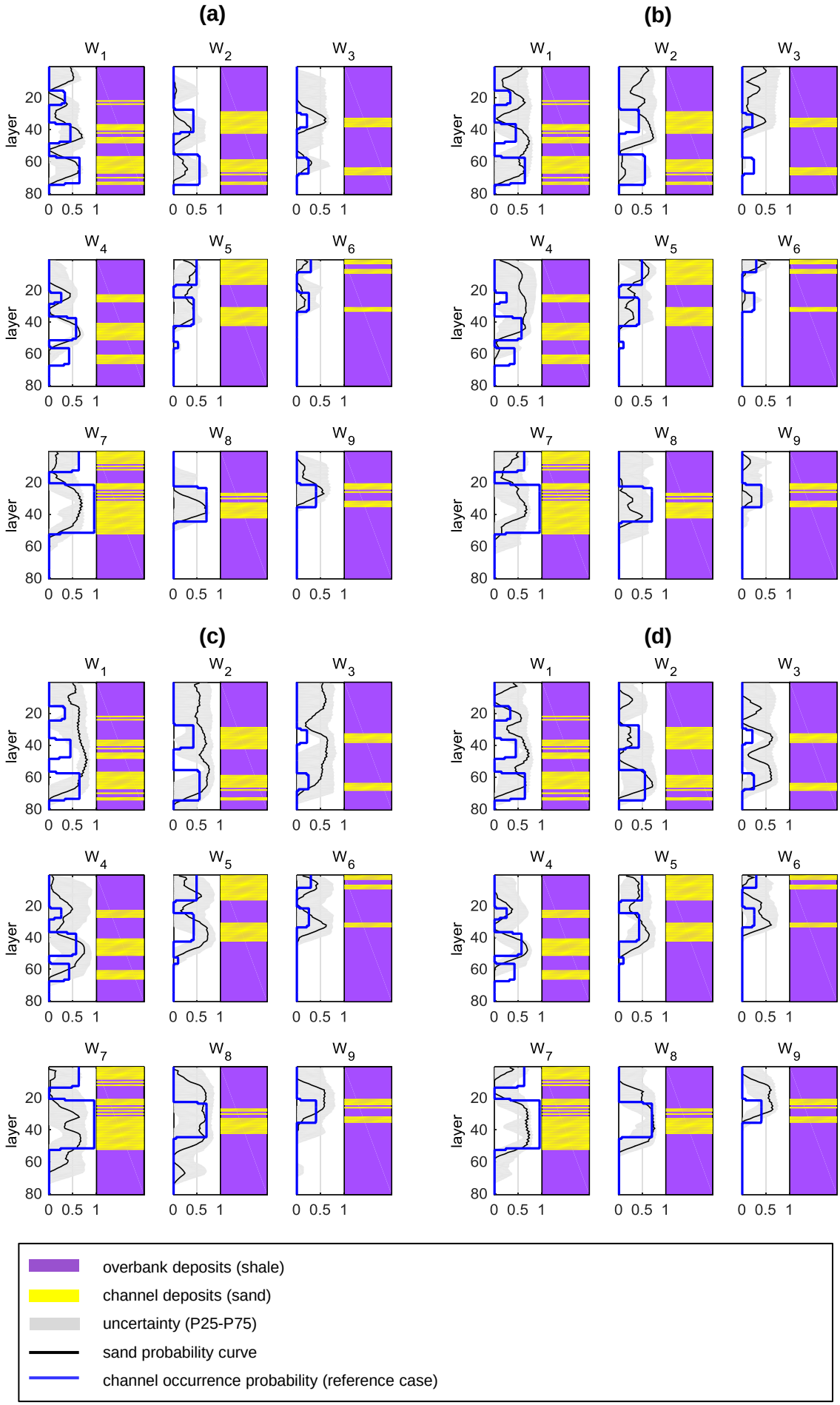
(a)
(b)
(c)
(d)
W1
W2
W3
W4
W5
W6
W7
W8
W9
layer
20
40
60
80
0 0.5 1
overbank deposits (shale)
channel deposits (sand)
uncertainty (P25-P75)
sand probability curve
channel occurrence probability (reference case)